ANL/RTR-15/9

Overview and Current Status of Analyses of Potential LEU Design Concepts for TREAT

Nuclear Engineering Division

About Argonne National Laboratory

Argonne is a U.S. Department of Energy laboratory managed by UChicago Argonne, LLC under contract DE-AC02-06CH11357. The Laboratory's main facility is outside Chicago, at 9700 South Cass Avenue, Argonne, Illinois 60439. For information about Argonne and its pioneering science and technology programs, see www.anl.gov.

DOCUMENT AVAILABILITY

Online Access: U.S. Department of Energy (DOE) reports produced after 1991 and a growing number of pre-1991 documents are available free via DOE's SciTech Connect (http://www.osti.gov/scitech/)

Reports not in digital format may be purchased by the public from the National Technical Information Service (NTIS):

U.S. Department of Commerce
National Technical Information
Service 5301 Shawnee Rd
Alexandria, VA 22312
www.ntis.gov
Phone: (800) 553-NTIS (6847) or
(703) 605-6000
Fax: (703) 605-6900
Email: orders@ntis.gov

Reports not in digital format are available to DOE and DOE contractors from the Office of Scientific and Technical Information (OSTI):

U.S. Department of Energy
Office of Scientific and Technical Information
P.O. Box 62
Oak Ridge, TN 37831-0062
www.osti.gov
Phone: (865) 576-8401
Fax: (865) 576-5728
Email: **reports@osti.gov**

Disclaimer

This report was prepared as an account of work sponsored by an agency of the United States Government. Neither the United States Government nor any agency thereof, nor UChicago Argonne, LLC, nor any of their employees or officers, makes any warranty, express or implied, or assumes any legal liability or responsibility for the accuracy, completeness, or usefulness of any information, apparatus, product, or process disclosed, or represents that its use would not infringe privately owned rights. Reference herein to any specific commercial product, process, or service by trade name, trademark, manufacturer, or otherwise, does not necessarily constitute or imply its endorsement, recommendation, or favoring by the United States Government or any agency thereof. The views and opinions of document authors expressed herein do not necessarily state or reflect those of the United States Government or any agency thereof, Argonne National Laboratory, or UChicago Argonne, LLC.

ANL/RTR-15/9

Overview and Current Status of Analyses of Potential LEU Design Concepts for TREAT

Prepared by
H. M. Connaway, D. C. Kontogeorgakos, D. D. Papadias, and A. E. Wright
Nuclear Engineering Division, Argonne National Laboratory

Sponsored by
U. S. Department of Energy, National Nuclear Security Administration
Office of Material Management and Minimization

October 2015

Executive Summary

Neutronic and thermal-hydraulic analyses have been performed to evaluate the performance of different low-enriched uranium (LEU) fuel design concepts for the conversion of the Transient Reactor Test Facility (TREAT) from its current high-enriched uranium (HEU) fuel. TREAT is an experimental reactor developed to generate high neutron flux transients for the testing of nuclear fuels.

The goal of this work was to identify an LEU design which can maintain the performance of the existing HEU core while continuing to operate safely. A wide variety of design options were considered, with a focus on minimizing peak fuel temperatures and optimizing the power coupling between the TREAT core and test samples. Designs were also evaluated to ensure that they provide sufficient reactivity and shutdown margin for each control rod bank.

Analyses were performed using the core loading and experiment configuration of historic M8 Power Calibration experiments (M8CAL). The Monte Carlo code MCNP was utilized for steady-state analyses, and transient calculations were performed with the point kinetics code TREKIN. Thermal analyses were performed with the COMSOL multi-physics code.

Using the results of this study, a new LEU Baseline design concept is being established, which will be evaluated in detail in a future report.

Table of Contents

Page

Executive Summary iv

Table of Contents v

List of Figures vii

List of Tables viii

1 Introduction 1

2 Analysis Overview 1

2.1 Summary of TREAT Design and Operation 1
2.2 Core Conversion Requirements 2
2.3 Current Methodology 3
2.3.1 Core Loading 3
2.3.2 Code System 4
2.3.3 Accident Scenario 5

3 LEU Analyses - Early Scoping Studies 5

3.1 Fuel Graphitization 6
3.2 Fuel-to-clad Gap Studies 6
3.3 Axial Grading of Fuel Materials 8
3.4 Reflectors Placed Near the Test Region 9

4 LEU Analyses - Variant 1 Series 10

5 LEU Analyses - Variant 2 Series 14

5.1 Initial Neutronic Evaluation 14
5.2 Thermal-hydraulic Evaluation of Baseline 2.0 and Variant 2.n Designs 16
5.2.1 Baseline 2.0 and Variant 2.1-2.3 Peak Fuel and Cladding Temperatures 18
5.2.2 Gap between Cladding and Reflector, Baseline 2.0 and Variants 2.n 19
5.2.3 Zircaloy Emissivity, Variant 2.1 20
5.2.4 Core Energy and Temperature Behavior, Variant 2.1 21
5.3 Variant 2.1 Detailed Analysis 22
5.3.1 Variant 2.1 Summary 22
5.3.2 Variant 2.1 Transient Behavior 22
5.3.3 Variant 2.1 Accident Analysis 22
5.3.4 Steady-state Evaluation of Additional Experiments in the Variant 2.1 LEU Core 29

6 LEU Analyses - Baseline 3 30

6.1 Baseline 3.0 Reference Behavior 30
6.2 Baseline 3.0 Sensitivity Study 31
6.3 Baseline 3.1 with BeO 33
6.4 Baseline 3.1 with Inconel Cladding on Select Assemblies 35

7 Re-baselining the LEU Design 36

7.1 June 2015 Reference Design 36
7.2 Perturbations of June 2015 Reference Design 39

8 Conclusions and Future Work 40

References 42

List of Figures

Page

Figure 1. Control Rod Positions with the TREAT Core 2
Figure 2. Illustration of TREAT Transients, (a) Shaped Transient and (b) Temperature-limited Transient .. 2
Figure 3. M8CAL ½-slotted Core Loading 4
Figure 4. Core Loading with Axially-graded Fuel Assemblies in (Orange) Select Locations 8
Figure 5. Relative Power Distribution when Different C/U Ratios are Used Axially 9
Figure 6. LEU Variant 2 Series Designs 15
Figure 7. Axial and Cross-sectional Geometric Details of the Baseline 2.0 and Variant 2.n Designs 17
Figure 8. Locations Where Peak Cladding Temperatures were evaluated for LEU Baseline 2.0 and Variant 2.n Designs 18
Figure 9. Peak Fuel and Cladding Temperatures at Side for 12.7 MJ Transient, Baseline 2.0 and Variants 2.1-2.3 with Cooling 19
Figure 10. Temperature of the Cladding at the Side Wall as a Function of Time and Vacuum Gap Distance into the Reflector, for Variant 2.1 in a 12.7 MJ Transient with Cooling; LR = Lower Reflector and UR = Upper Reflector 20
Figure 11. Effect of Zircaloy Emissivity on Peak Cladding Temperature for Variant 2.1, for 12.7 MJ Transient with Constant Peak Fuel Temperature of 617°C and Forced Air Cooling 21
Figure 12. Relationship Between Peak Fuel Temperature and Peak Cladding Temperature, for Variant 2.1 with Cooling 21
Figure 13. Temperature Reactivity Feedback vs. Core Energy for HEU and LEU Variant 2.1 M8CAL Half-slotted Core 23
Figure 14. Maximum Shaped Transient, for Equal TED, in HEU and LEU Variant 2.1 24
Figure 15. Power-time History of the Maximum Reactivity Insertion Accident in the LEU Variant 2.1 Core 25
Figure 16 - Cooling Time History for LEU Variant 2.1 During an Accident-Case Scenario, With Air Flow (Upper Graph) and Without Air Flow (Lower Graph) 28
Figure 17. LO3 Experiment Configuration Used in HEU and LEU MCNP Simulations 29
Figure 18. S11 and S12 Experiment Configuration Used in HEU and LEU MCNP Simulations, (a) X-Z View and (b) X-Y View 30
Figure 19. Locations (in Orange) where Inconel Cladding Was Tested in the Baseline 3.1 TREAT LEU Core 36
Figure 20. Bounding Shaped Transient, for Equal TED, in HEU and June 2015 LEU Reference Design 38
Figure 21- Cooling Time History for June 2015 LEU Reference Design During an Accident Case Scenario with No Air Flow 39
Figure 22. Illustration of the Challenge in Engineering Design Changes to Resolve LEU PCF < HEU PCF in Operations with Coolant Flow 41

List of Tables

Page
Table 1. LEU Scoping Studies – Impact of Graphitization 6
Table 2. LEU Scoping Studies – Impact of Gap Size 7
Table 3. LEU Scoping Studies – Graphite in Gap 7
Table 4. LEU Scoping Studies – Microporous Insulation in 1/8-in Gap 8
Table 5. Results Utilizing Moderating Elements Near the Test Vehicle 10
Table 6. Key Design Parameters in LEU Variant 1 Series Analyses 11
Table 7. Key Results for LEU Variant 1 Series Analyses 11
Table 8. LEU Variant 1 Series - Estimated Energy and Peak Fuel Temperature to match HEU Energy of 3000 MJ 13
Table 9. Variant 1 Series Results – Control Rod Bank Worths 13
Table 10. Temperature Reactivity Feedback – HEU Core and LEU Baseline 1.0 14
Table 11. Summary of Variant 2 Design Parameters 14
Table 12. All-rods-out Excess Reactivity in Variant 2 Series Designs 15
Table 13. Parameters used in the Thermal-hydraulic Evaluations of the Baseline 2.0 and Variant 2.n LEU Designs 16
Table 14. Peak Fuel and Cladding Temperatures for 12.7 MJ Transient with Cooling, LEU Baseline 2.0 and Variants 2.1-2.3 18
Table 15. All-Rods-Out Excess Reactivity and Control Rod Bank Worth in LEU Variant 2.1 Core 22
Table 16. Kinetic Properties of LEU Variant 2.1 Core 23
Table 17. Bounding Shaped Transient, for Equal TED, in HEU and LEU Variant 2.1 23
Table 18. Behavior if Initial Available Reactivity of Bounding Shaped Transient (for Equal TED) is inserted as a Step, with no Cooling, for HEU and LEU Variant 2.1 24
Table 19. Estimates of Peak Temperature for Different LEU/HEU PCF Values 24
Table 20. Heat Capacity as a Function of Temperature for Zircaloy-2 26
Table 21. Peak Fuel and Cladding Temperatures for Variant 2.1 Accident Scenario Under Different Conditions 27
Table 22. Peak Cladding Temperature and Cooling Time for Variant 2.1 Accident Scenario with Coolant Flow 28
Table 23. Peak Cladding Temperature and Cooling Time for Variant 2.1 Accident Scenario with No Coolant Flow 28
Table 24. Key Results for LEU Designs Baseline 3.0 and Variant 2.1 31
Table 25. Parameters Evaluated in Baseline 3.0 Sensitivity Study 31
Table 26. LEU Baseline 3.0 Sensitivity Study Results – Boron Impurity and Density 32
Table 27. LEU Baseline 3.0 Sensitivity Study Results – Graphitization, C/U, and Enrichment 32
Table 28. LEU Properties Used to Investigate Further Improvement of Baseline 3.0 33
Table 29. Results Investigating Further Improvement of Baseline 3.0 33
Table 30. LEU Composition for Baseline 3.1 with BeO Reflectors 34
Table 31. Reactivity and Control Rod Bank Worths for Baseline 3.1 with BeO Reflectors 34
Table 32. LEU/HEU PCF for Baseline 3.0 with BeO Reflectors 34
Table 33. Peak Fuel Temperature with Equal Core Energy, for Baseline 3.1 with BeO Reflectors 35
Table 34. Inconel Composition Used in Baseline 3.1 Cladding Analysis 35

Table 35. Behavior of June 2015 Reference LEU Design Geometry for Different C/U Ratios 37
Table 36. Key Results for June 2015 LEU Reference Design with C/U=2150 37
Table 37. Transient Results for June 2015 LEU Reference Design 38
Table 38. Sensitivity Study of the June 2015 Reference Design 40

1 Introduction

The Transient Reactor Test Facility (TREAT) is an experimental reactor located at Idaho National Laboratory (INL). It was developed for experimental testing of the transient behaviors of reactor fuels and other materials. TREAT first became critical in 1959 and was used to perform hundreds of experiments before being placed on non-operational standby in 1994. The restart of TREAT is now being pursued under the U.S Department of Energy's (DOE) Resumption of Transient Testing Program. In addition, work is underway for the conversion of TREAT from its current high enriched uranium (HEU) fuel to low-enriched uranium (LEU)-bearing fuel, in keeping with the mission of the DOE National Nuclear Security Administration (NNSA) Material Management and Minimization (M^3) reactor conversion program.

Initial neutronic evaluation of an LEU core was presented in a June 2013 study [1]. Following this study, a number of additional design options have been evaluated by analysts at Argonne National Laboratory (ANL), in collaboration with the design team at INL and Los Alamos National Laboratory (LANL). This report summarizes the evolution in LEU fuel design, including neutronic and thermal-hydraulic results. Additional details on the thermal behavior of some of the LEU designs can be found in an accompanying report [2]. From the analyses outlined below, a new LEU baseline design is being established, which will be evaluated in a forthcoming report.

2 Analysis Overview

2.1 Summary of TREAT Design and Operation

TREAT is a homogenous, air-cooled, graphite-moderated and graphite-reflected reactor currently fueled with 93% enriched UO_2 dispersed in graphite with a fuel carbon to uranium-235 (C/U^{235}) ratio of approximately 10000:1. The reactor cavity can accommodate a maximum 19x19 array of fuel assemblies, which are each approximately 4-inch x 4-inch square x 9 feet long (with a central ~4 foot fuel region, and ~2 foot long graphite reflector regions above and below this, plus end fittings). A detailed description of the TREAT facility and current HEU fuel assembly design can be found in previous reports [1, 3]. During irradiation experiments, a small number of TREAT fuel assemblies (typically 2-4) at the core center are replaced with an experiment vehicle containing the test sample(s). In addition, a central row of fuel assemblies is frequently removed to provide an unimpeded path for neutrons between the test sample and an ex-core collimator and detector system called the hodoscope.

The TREAT core contains three different types of B_4C-bearing reactor control rods: (1) four pairs of control/shutdown rods used to set the reactor to a critical state, (2) four pairs of transient rods, whose motion is used for reactivity insertion, and (3) four compensation rods used for reactivity compensation when an experiment vehicle is removed. The current layout of these rods within the TREAT core is shown in Figure 1. The location of the control rods was reconfigured in the late 1980s; the current layout is referred to as the "upgraded core", while the previous configuration is identified as the "pre-upgrade core".

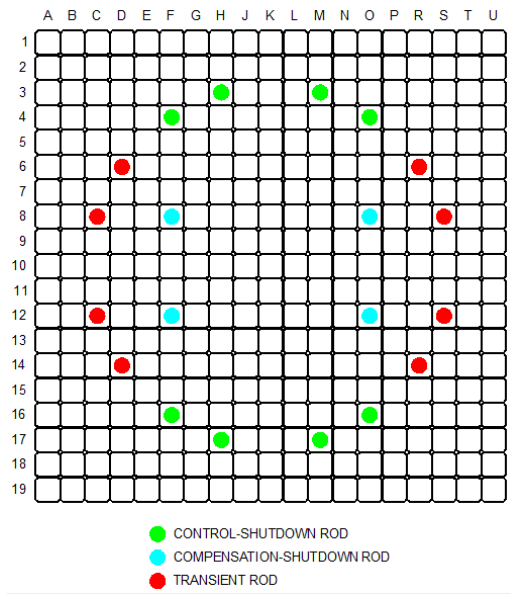

Figure 1. Control Rod Positions with the TREAT Core

Two different types of transients can be performed via motion of the transient rods: (1) shaped transients, in which a specific desired power-time history is produced using complex motions of the transient rods, and (2) temperature-limited transients, in which a step reactivity insertion is performed by withdrawing the transient rods at their maximum speed, causing a bell-shaped power "burst". The burst is controlled by the large, prompt, negative temperature reactivity feedback provided by the fuel graphite. An illustration of the two transient types is provided in Figure 2.

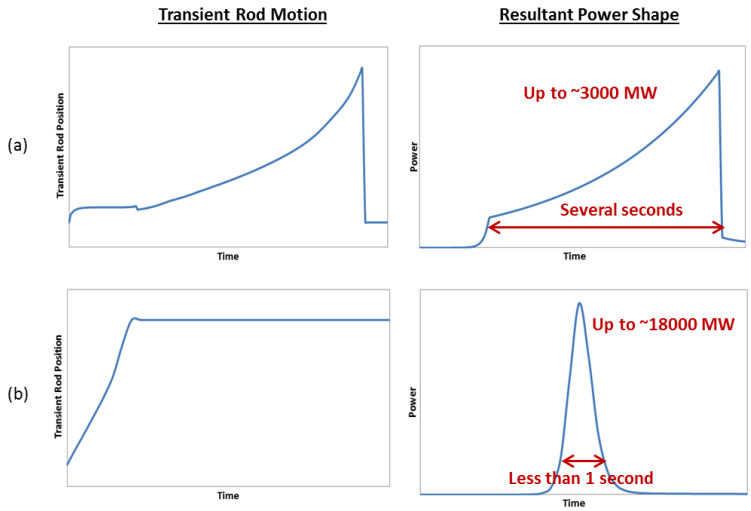

Figure 2. Illustration of TREAT Transients, (a) Shaped Transient and (b) Temperature-limited Transient

2.2 Core Conversion Requirements

For an LEU conversion of TREAT to be feasible, the converted core must maintain the reactor's experimental capabilities, while continuing to operate safely. A key performance metric is the ability to match the total energy deposition (TED) in a given test sample. The TED can be expressed in terms of core operation through a parameter called the power coupling factor (PCF), which represents the ratio

of test sample power (or energy) per unit mass to total reactor power (or energy). If the LEU core has a lower PCF than the HEU core for a given test sample, this means that more core energy is needed to achieve the same sample TED.

It is also important that the LEU fuel provides an appropriate amount of reactivity. There must be sufficient core all-rods-out (ARO) excess reactivity to compensate for the highest negative worth experiment vehicles and for the negative feedback in the most demanding transients. At the same time, the reactivity cannot be so high that the control rods are unable to make the core subcritical with sufficient margin.

Test sample TED and core reactivity were treated as the primary performance requirements during this stage of the conversion analysis. However, additional requirements may be evaluated in the future as the LEU design is finalized.

From a safety standpoint, a key parameter is the peak temperature experienced by the TREAT fuel assembly cladding. The temperature limits of the cladding (which are in place to minimize oxidation and prevent material phase change) are the limiting factors which dictate allowable TREAT operation. In the HEU core, there is a temperature limit during normal operation (Limiting Safety System Setting, or LSSS) of 600°C, and an accident scenario temperature limit (Safety Limit, or SL) of 820°C. To provide additional margin for thermocouple uncertainties, the 600°C limit was imposed as a 575°C limit during actual operation. The converted LEU core therefore must be able to match HEU core performance for any transient possible in the HEU core within these temperature limits. In the early analyses, there was a focus on minimizing peak cladding temperature under normal operating conditions, during which there is cooling air flow. However, it was later established that the focus should be on minimizing peak temperatures in the accident case, during which there is assumed to be no air flow.

2.3 Current Methodology

2.3.1 Core Loading

The different LEU designs were evaluated using the half-slotted core loading of the M8 power calibration experiment (M8CAL) [4]. M8CAL, performed in 1990-1993, is the latest, best-documented set of experiments done in the TREAT HEU core. The core loading (total uranium mass) is illustrated in Figure 3, with the test sample positioned at the center of the core. Early analyses focused on irradiation of the two M8CAL test pins, T-433 and T-462, which were made of highly enriched U-Zr and U-Pu-Zr respectively. Later analyses evaluated LEU performance for both pin T-462 and a hypothetical low-enriched test pin.

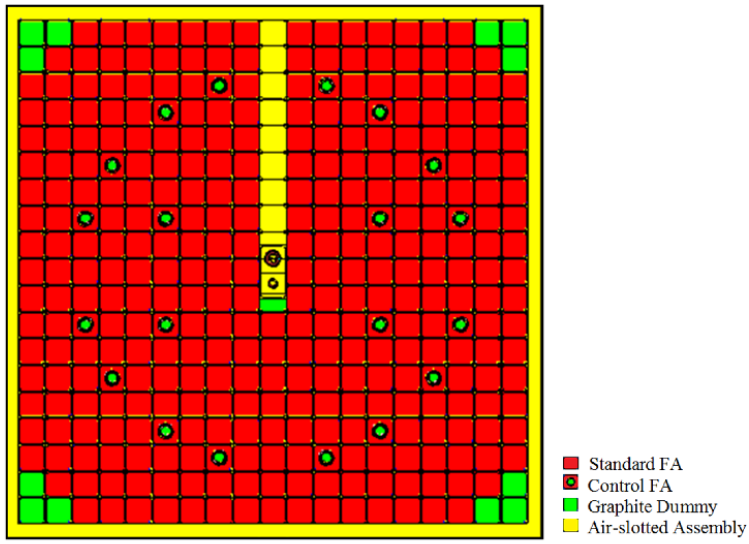

Figure 3. M8CAL ½-slotted Core Loading

2.3.2 Code System

Steady-state neutronic simulations were performed using the Monte Carlo code MCNP5, with ENDF/B-VII.0 cross-section data [5]. MCNP models of the existing HEU core have been benchmarked against historic irradiation experiments and the Minimum Critical Core experiments [3, 6]. Transient simulations were performed with TREKIN, a point kinetics code that was historically used during TREAT operations to evaluate transient behavior and support the design of experiments. TREKIN has been resurrected and updated for analysis of TREAT transients in an Excel-based input and output environment [7]. Its use requires input of a set of core-specific parameters: temperature reactivity feedback and core-average and hot-spot temperature values as functions of total core energy, transient bank available reactivity as a function of axial position, and the delayed neutron fraction and prompt generation lifetime. Historically this information came from measurements in the HEU core, but a method of generating the data with MCNP has been developed and validated using data from M8CAL, as well as an additional experiment series, ANCAL [8, 9]. Temperature reactivity feedback is calculated using hot core cross-section data generated with the makxsf MCNP utility program [10]. The temperature distributions for these simulations are estimated based on MCNP-calculated cold core power distributions. Analyses to investigate the impact of rod position on power distribution and temperature reactivity feedback are underway. The fuel UO_2-graphite is treated as a homogenous mixture in the analysis models. Evaluation of fuel transient behavior on the particulate level was performed in separate studies by Mo, et al. [11].

Thermal-hydraulic analyses have been performed using the multi-physics finite element software COMSOL® V 3.5a. In order to verify the model and methodology, a 3D single-assembly model for the HEU core was developed and benchmarked against historic TREAT analysis results, as outlined in an accompanying report [2]. This additional report also provides details on the thermal properties assumed in the modeling.

2.3.3 Accident Scenario

As indicated above, early phases of the work focused on identifying design features that minimize peak cladding temperature during normal operation with cooling air flow. However, as further understanding of the HEU safety basis developed, it became clear that the focus should instead be on a no-flow reactivity insertion accident scenario, which closely corresponds to the maximum fuel temperature which a fuel assembly must be able to withstand.

The TREAT administrative safety limit (SL) of 820°C represents the peak allowable cladding temperature that can be experienced by any fuel assembly under an accident in which there is an accidental insertion of reactivity, the cooling air-blowers fail, and free-convection air circulating through the core is prevented. Therefore, allowable transients under normal operation are limited to those which would remain below this SL temperature limit in accident conditions. Operationally, this is a constraint on the allowable available reactivity, or allowable pre-transient position of the transient rod bank. The accident scenario assumes that the step reactivity insertion occurs prior to the start of a planned transient, and that the full reactivity available for the planned transient is inserted. For the HEU M8CAL half-slotted core, this reactivity limit was 5.95%Δk/k.

To evaluate the accident scenario in the LEU core, the first step taken was to calculate an HEU shaped transient using the maximum allowable reactivity, which represents the HEU core under normal operation. This is done using the period-driven mode in TREKIN, for a 0.3 second initial period, and then a period change at t = 2.8 seconds to an 8-second period, with 5.95% initial reactivity for the transient. The HEU accident scenario was then evaluated by performing a step reactivity insertion (i.e., maximum speed rod withdrawal) of this same 5.95% reactivity. This creates a temperature-limited transient which approaches the 820°C limit. To meet the conversion requirement, the LEU core must be able to match the test-sample TED achievable in the evaluated 5.95% reactivity HEU shaped transient. The LEU-core shaped transient necessary to accomplish this is estimated by scaling the HEU-core shaped transient power-time history by a multiplying factor equal to the ratio of the PCFs in the two cores. The resultant LEU power-time history is evaluated using the TREKIN power-driven mode to determine the pre-transient reactivity (i.e., pre-transient rod position) needed. Finally, the LEU accident scenario is calculated assuming a step insertion of this reactivity. As described above, each of the transient simulations is performed using TREKIN.

For evaluation of the fuel assembly temperatures during the reactivity accident, the TREKIN-calculated power-time history and MCNP-calculated core relative power distributions are then used for COMSOL simulations. This analysis provides detailed information on the temperature profile of the fuel and cladding, including peak cladding temperature (which, as described above, is the key parameter of interest in the accident).

3 LEU Analyses - Early Scoping Studies

The first phase of the analysis was a broad scoping study in which a large variety of options were explored. The list of concepts considered in this study was developed in a meeting between INL and ANL in January 2014. The goal of this work was to identify design features which (1) improve the PCF, and (2)

reduce the hot spot cladding temperature. Neutronic results for the scoping study are presented below, and thermal-hydraulic results can be found in an accompanying report [2].

The various studies were performed starting from a "reference" LEU design which had a total fuel density of 1.75 g/cm^3, 2 ppm boron equivalent impurity (modeled as 2 ppm natural boron), 59% graphitization (same as HEU), 19.75% ^{235}U enrichment (balance assumed to be ^{238}U at this stage in the analysis), and a C/U ratio of 1400. This C/U is larger than the value used in the previous studies [1]. This is because the older analyses assumed that the LEU had the same level of boron impurity as the HEU, 7.6 ppm, making it necessary to have more uranium to achieve equal reactivity with the HEU M8CAL core. The LEU geometric design was assumed to be the same as in the HEU core. The LEU cladding is a zirconium-based alloy. Zircaloy-3 (which is used in the HEU core) was assumed in early analyses but was later changed to Zircaloy-4. Calculations were performed with the control rod banks placed in "Configuration A," one of the rod configurations used in M8CAL [4].

3.1 Fuel Graphitization

Three different LEU fuel graphitization values were simulated to examine their impact on PCF. As described in the HEU Minimum Critical Core studies [3], partial graphitization is accounted for in the neutronics simulations by applying S(α,β) treatment to the portion of the fuel carbon which is considered graphitized, and free-gas treatment to the un-graphitized portion. The results of this analysis are summarized in Table 1. For higher graphitization values the excess reactivity decreases and the PCF increases.

Table 1. LEU Scoping Studies – Impact of Graphitization

% graphitization	k_{eff}	(LEU PCF) / (HEU PCF)	Reactivity Difference from Reference, pcm
59%	1.01555	79.5%	/
70%	1.01278	80.4%	-269
80%	1.00990	81.6%	-551
90%	1.00636	82.8%	-899

3.2 Fuel-to-clad Gap Studies

At the time of the scoping studies, the analysis focus was on establishing design features which would reduce peak cladding temperatures under normal operation, during which there is cooling air flow. A number of design features were evaluated to support this, including an increased fuel-to-clad gap (external dimensions of the assembly are maintained, fuel block dimensions are reduced) and the placement of materials between the fuel and cladding. Both microporous insulation and pyrolytic graphite (which enhances heat transfer in a particular direction) were considered.

For this preliminary analysis, the density of the fuel was adjusted to compensate for changes in fuel volume and preserve the same total core mass. The goal in using this approach was to somewhat isolate the impact of the gap change, and to neglect effects on the core performance due to a loss of fuel material. It should be noted that this was merely a hypothetical approach taken for the analysis and does not represent reality (where the fuel density cannot exceed a practical physical limit).

Table 2 presents results for different air-filled gap sizes. Increasing the gap from 0.05” to a larger size of 1/8” causes a decrease in reactivity, but there is negligible change in PCF. Increasing further to 1/4", however, causes a large decrease in both reactivity and PCF. Recall as well that these results represent the behavior for equal core loading; if the same composition had been used in all cases, the reactivity decrease would be even larger. These results indicate that increasing the gap size causes an increase in axial neutron leakage, which leads to a loss of reactivity and a decrease in the proportion of core neutrons reaching the test sample.

Table 2. LEU Scoping Studies – Impact of Gap Size

Gap	(LEU PCF) (HEU PCF)	Reactivity Difference from Reference, pcm
Reference (0.050 in.)	79.5%	/
1/8”	78.7%	-599
1/4"	68.1%	-2023

A similar study was performed to evaluate placing graphite between the fuel and the cladding (Table 3). The analysis demonstrated that graphite placed around the fuel region acts as an individual reflector on each assembly, causing an increase in reactivity and a decrease in the portion of neutrons reaching the test sample (decrease in PCF). This effect is more pronounced for the thicker layer of graphite.

Table 3. LEU Scoping Studies – Graphite in Gap

Gap	(LEU PCF) (HEU PCF)	Reactivity Difference from Reference, pcm
Reference (50 mil, air)	79.5%	/
1/8” graphite	76.9%	4838
1/4" graphite	74.3%	8290

Several different microporous insulation materials were also evaluated, to examine the relative differences in their impact. Each material was evaluated assuming a 1/8” layer placed between the fuel and clad. The results are summarized in Table 4.. None of the microporous insulation options cause a significant change in PCF. All of the materials cause a roughly 500 pcm decrease in reactivity (again assuming an increased fuel density to maintain the same loading), with the exception of the mixtures containing TiO_2, which causes significantly more reactivity loss.

Table 4. LEU Scoping Studies – Microporous Insulation in 1/8-in Gap

Insulating Material	(LEU PCF) / (HEU PCF)	Reactivity Difference from Reference, pcm
75% SiO_2, 25% Al_2O_3	79.0%	-485
75% SiO_2, 25% CaO_3Si	79.1%	-590
55% SiO_2, 45% $ZrSiO_4$	79.6%	-494
100% SiO_2	79.3%	-554
95% SiO_2, 5% SiC	78.8%	-489
50% SiO_2, 50% SiC	79.4%	-570
90% SiO_2, 10% TiO_2	79.8%	-1603
50% SiO_2, 50% TiO_2	79.0%	-6050

3.3 Axial Grading of Fuel Materials

In an effort to reduce the axial hot-spot power peaking, analyses were done to evaluate an axial grading of the C/U within the fuel. The goal of this approach was to drive the power away from the hottest location in the assembly.

As a trial case, simulations were performed using axially-graded assemblies in the hottest locations within the core (indicated in orange in Figure 4). These assemblies utilized a C/U of 1539 in the central 20% of the fuel region, and a C/U of 1370 in the upper and lower 40% of the fuel, with a density of 1.75 g/cm^3 and boron impurity of 2 ppm in all regions. These values were selected to preserve the total loading of a reference design fuel assembly ($U_{upper} + U_{lower} + U_{central} = U_{reference}$).

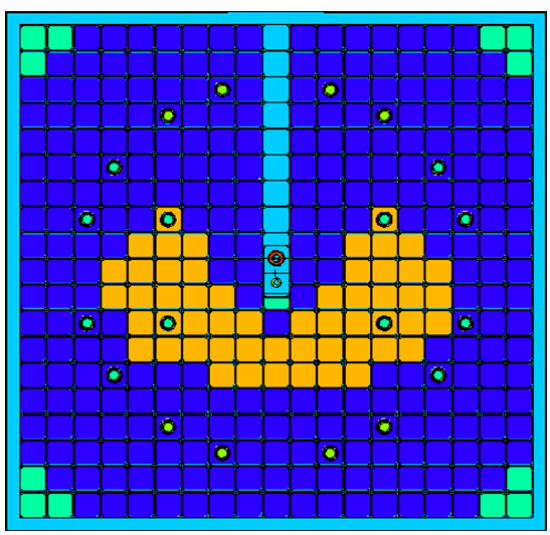

Figure 4. Core Loading with Axially-graded Fuel Assemblies in (Orange) Select Locations

Applying an increased C/U ratio did indeed reduce the power profile at the axial center of the fuel. However, this change also created peaks at the interfaces of the composition regions (Figure 5). Additional changes could be made to make the transition in composition more gradual, which could help to reduce this peaking. However, it would be very challenging to determine an optimized axial

distribution of material because the axial power profile changes with control rod position. Therefore, it was decided that this concept is not worth pursuing at this time.

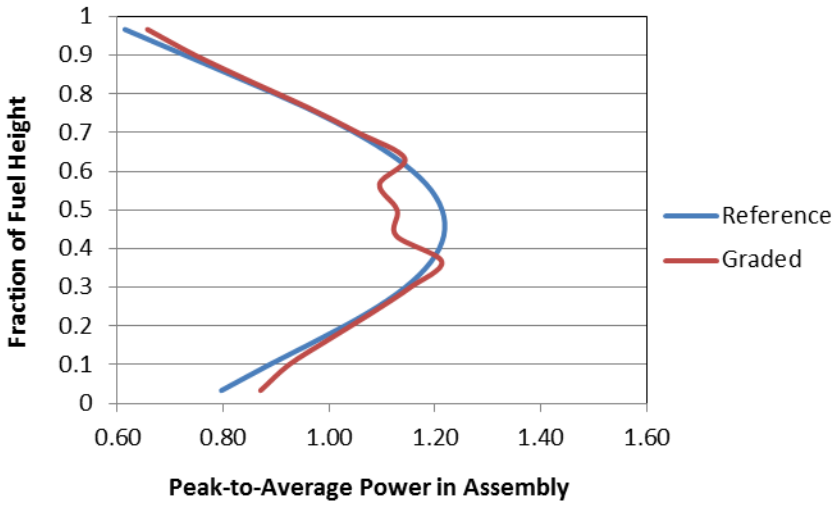

Figure 5. Relative Power Distribution when Different C/U Ratios are Used Axially

3.4 Reflectors Placed Near the Test Region

To investigate further improvement in the LEU core PCF, simulations were also performed using BeO and graphite dummy elements in locations adjacent to the experiment vehicle. These materials serve to further thermalize neutrons before they reach the test sample, creating a neutron spectrum that is more favorable for causing fissions in the sample. The benefits of using BeO have been demonstrated already in previous studies [1]. Additional cases were also studied by increasing the length of the fuel region to 5 ft. in locations where the highest temperature were expected. The analyses are summarized in Table 5. For an illustration of the stated core locations (J8, L8, etc.), please refer back to Figure 1. The power peaking factor (PPF) was also calculated as the ratio of the maximum local power density and the core average power density.

The presence of moderator material (graphite, Be, BeO) around the test vehicle enhances the thermal part of the neutron spectrum reaching the test vehicle, and an increase of the PCF is observed (cases 2-4). The power density in the fuel assemblies adjacent to the moderating blocks is also increased, so higher temperatures are expected. To address this issue, fuel assemblies with 5-foot fuel section and lower U-235 loading were considered for those locations (cases 5-8).

Table 5. Results Utilizing Moderating Elements Near the Test Vehicle

	Changes from Reference Core	(LEU PCF) (HEU PCF)	Reactivity Diff. from Ref., pcm	PPF
1	• (Reference Results)	79.5%	/	1.79
2	• Four Graphite Elements, in J9, J10, L9, and L10	84.0%	-427	1.77
3	• Four Be Elements, in J9, J10, L9, and L10	89.6%	-29	1.89
4	• Four BeO Elements, in J9, J10, L9, and L10	88.5%	-41	1.75
5	• Four BeO Elements, in J9, J10, L9, and L10 • Eight 5 ft FAs, in J8, L8, H9, M9, H10, M10, J11, L11 • Reference Composition in 4 ft FAs and 20% Lower Loading in 5 ft FAs to Retain Reference Core Net Loading	87.8%	-301	1.57
6	• Four BeO Elements, in J9, J10, L9, and L10 • Eight 5 ft FAs in J8, L8, H9, M9, H10, M10, J11, L11 • Reference Composition in 5 ft FAs, Reduced Loading in 4 ft FAs to Retain Reference Core Net Loading	88.4%	-183	1.80
7	• Four BeO Elements, in J9, J10, L9, and L10 • Twelve 5 ft FAs in H8, J8, L8, M8, H9, M9, H10, M10, H11, J11, L11, M11 • Reference Composition in 5 ft FAs, Reduced Loading in 4 ft FAs to Retain Reference Core Net Loading	89.6%	-299	1.80
8	• Four BeO Elements, in J9, J10, L9, and L10 • Twelve 5 ft FAs in H8, J8, L8, M8, H9, M9, H10, M10, H11, J11, L11, M11 • Reference Composition in 5 ft FAs, Reduced Loading in 4 ft FAs to Retain Reference Core Net Loading • Graphitization Increased 59% -> 80%	91.0%	-804	1.79

4 LEU Analyses - Variant 1 Series

Following the preliminary scoping work, seven INL-proposed LEU designs, referred to as Baseline 1.0 and Variants 1.1 – 1.6, were evaluated in greater detail. The key fuel design parameters are summarized in Table 6. All of these cases were evaluated with a fuel C/U of 1452, boron impurity of 2 ppm, and density of 1.75 g/cm^3. Baseline 1.0 - Variant 1.3 featured a 50 mil fuel-to-clad dimension, while in Variants 1.4, 1.5, and 1.6 the fuel volume was reduced to accommodate the added materials (micro-porous insulator and/or pyrolytic graphite). In Variant 1.3, all of the parameters are identical to Baseline 1.0 except that some of the cladding is assumed to be in contact with the fuel. This is important in the thermal analysis, but neutronically, these two cases are the same, so in the MCNP calculations the gap was maintained at 0.05" around the fuel. The Variant 1.n series designs featured the same cladding thickness and radial fuel block dimensions as the HEU fuel assembly. However, unlike the HEU assembly, these designs feature a single continuous Zircaloy cladding over the fuel and axial reflectors, with no axial spacers between the fuel and reflector regions. Detailed thermal-hydraulic evaluations of the LEU Variant 1 series designs can be found in a separate report [2].

Table 6. Key Design Parameters in LEU Variant 1 Series Analyses

Parameter	Current HEU	Baseline 1.0	Variant 1.1	Variant 1.2	Variant 1.3	Variant 1.4	Variant 1.5	Variant 1.6
C/U_{total}	9257	1452	1452	1452	1452	1452	1452	1452
Density (g/cm^3)	1.73	1.75	1.75	1.75	1.75	1.75	1.75	1.75
Graphitization	59%	70%	70%	85%	70%	70%	70%	70%
Boron	7.6	2.0	2.0	2.0	2.0	2.0	2.0	2.0
Core length (ft)	4	4	5	4	4	5	5	5
Fuel-clad gap(inches)	0.05	0.05	0.05	0.05	0.05	0.05	0.05	0.05
Insulator	none	none	none	none	none	none	1/16"	1/16" *
PyG	none	none	none	none	none	1/8" *	1/16" *	1/16"

* in contact with the fuel meat

Key results from each case are summarized in Table 7. HEU core results are also provided for comparison. The HEU core was simulated in a reported historic critical rod configuration, with the control/shutdown rod bank 50% withdrawn and the transient and compensation/shutdown banks fully withdrawn. A similar LEU core rod configuration with the control/shutdown rods 47% withdrawn was selected for Baseline 1.0 to yield a similar k-effective value. This rod configuration was then used for simulating all LEU Variant 1 series cases. Peak fuel temperature values are listed assuming a fixed core energy value of 3000 MJ in all cases (but in reality the different designs would require different core energy values, as discussed below). These values assume adiabatic heating of the fuel assemblies, and the temperature distribution is based on the MCNP-calculated cold core power distribution. Additional detail on this method can be found in an accompanying report [8].

Table 7. Key Results for LEU Variant 1 Series Analyses

Parameter	Current HEU	Baseline 1.0 & Variant 1.3	Variant 1.1	Variant 1.2	Variant 1.4	Variant 1.5	Variant 1.6
Design Change from 1.0	-	-	5ft core	85% grph	5ft core, PyGr	5ft core, PyGr/MP	5ft core, MP/PyGr
(k-1)/k, pcm	2790	3496	6941	3085	6882	3074	3403
Peak Fuel Temp* (°C)	638	612	546	610	611	588	593
(LEU PCF)/ (HEU PCF)	-	81%	68%	82%	74%	75%	75%
PPF	1.78	1.69	1.82	1.69	1.88	1.78	1.80
l_p (μs)	855	764	692	771	(did not calculate)		
b_{eff}	0.0068	0.0068	0.0068	0.0069			

* Assuming equal total core energy

Several conclusions can be drawn from the results of the Variant 1 series analyses. For the same amount of core energy, the peak fuel temperature in a 5-foot core is lower than that in a 4-foot core. However, the PCF of the 5-foot core is also significantly lower. This means that more core energy is needed for the same TED, and therefore the peak temperature values listed in Table 7 are not representative to true operating core behavior. The 5-foot core also exhibits too much excess reactivity with the Variant 1 fuel composition. Therefore, this geometry would only be feasible with an increased C/U ratio. Variant 1.4 - 1.6 results indicate that for the same fuel block geometry, the orientation of the insulation and pyrolytic graphite does not significantly affect PCF. But this does affect power peaking, and consequently also affects peak fuel temperature (for the same core energy). As demonstrated in the corresponding thermal analyses, these materials do also help to reduce peak cladding temperatures only if air flow for cooling is present [2].

In order to evaluate the peak fuel temperatures more realistically, an energy factor was calculated for each design as the ratio of the cold, critical core HEU-to-LEU PCF. This ratio estimates the relative core energy increase needed in the LEU core to achieve the HEU core TED. For a given HEU core energy, the corresponding core energy needed in each LEU design was determined as the multiple of the energy factor and HEU core energy:

$$TED_{HEU} = TED_{LEU} \rightarrow [PCF_{HEU} * Energy_{HEU}] = [PCF_{LEU} * Energy_{LEU}]$$

$$\rightarrow Energy_{LEU} = \left[\frac{PCF_{HEU}}{PCF_{LEU}} * Energy_{HEU}\right] = [(Energy\ Factor) * Energy_{HEU}]$$

It should be noted that this method provides a rough estimate, rather than a definitive value. In reality, the relationship between a test sample and the core changes during the course of a transient due to core temperature rise and control rod motion [12]. The magnitude of this change may differ between the HEU core and the LEU core, which means that the LEU core power-time history needed to match the power-time history of a test sample in the HEU core in reality is not a constant multiple of the HEU core power-time history. However, this approach is considered sufficient for the current stage of the analysis. The transient change in relationship between test sample and the LEU core will be evaluated in further detail once the LEU design is more finalized. The PCF will be evaluated as a function of core temperature in both the HEU and LEU cores for multiple experiment types. This information will be used to more accurately assess the core power-time history needed in the LEU core for a given desired sample behavior.

This approach is applied in Table 8, which presents as an example the LEU core energy values needed to match the TED obtained by an HEU core energy of 3000 MJ. Again assuming adiabatic heating of the fuel assemblies, the resulting hot-spot fuel temperatures were estimated using the MCNP-calculated cold-core power distribution. Table 8 indicates that the lowest temperature is achieved in Variant 1.2, the four-foot core with increased graphitization. This is also the case with the largest PCF value. It should be highlighted that the presented values represent fuel temperatures; the relative differences in the peak cladding temperatures will be different (during normal operation with cooling air flow) due to the design features present in some cases (insulation and/or pyrolytic graphite) which help to reduce cladding temperatures.

The calculated control rod bank worths for each LEU design are presented in Table 9, along with the calculated values for the HEU core. There is a decrease in the worth of the B_4C control rods relative to the HEU core for all of the Variant 1 cases. This is because the worth of the rods is related to the average neutron spectrum in the core – the harder the spectrum (i.e., the higher the average neutron energy), the lower the rod worth. In addition, the length of the poison section in the current control rods is 56.125" (4.677 feet). Therefore, the rods may need to be lengthened if the core height is increased to 5 feet. As mentioned previously, the 5-foot core cases (Variants 1.1 and 1.4) also provide far too much reactivity with the current composition and thus would require an adjustment in C/U.

Table 8. LEU Variant 1 Series - Estimated Energy and Peak Fuel Temperature to match HEU Energy of 3000 MJ

Core	PCF	Energy Factor	Energy Needed (MJ)	Calculated Hot Spot Temp (°C)
HEU	5.22	1.00	3000	638
LEU Var. 1.0 and 1.3	4.21	1.24	3719	716
LEU Var. 1.1	3.54	1.48	4426	724
LEU Var. 1.2	4.29	1.22	3646	704
LEU Var. 1.4	3.84	1.36	4078	765
LEU Var. 1.5	3.92	1.33	3997	725
LEU Var. 1.6	3.92	1.33	3987	730

Table 9. Variant 1 Series Results – Control Rod Bank Worths

Core	ARO Reactivity (%)	Rod Bank Worth (%)		
		Transient	Control/Shutdown	Compensation
HEU	7.8	9.1	9.4	8.5
Baseline 1.0	8.1	8.1	8.6	7.5
Variant 1.1	10.9	7.2	7.8	6.8
Variant 1.2	7.8	8.3	8.8	7.7
Variant 1.3	8.1	8.1	8.6	7.5
Variant 1.4	11.0	7.5	8.1	7.1
Variant 1.5	7.6	8.1	8.9	7.6
Variant 1.6	7.9	8.1	8.8	7.6

The harder neutron spectrum in the LEU core also causes a decrease in the temperature reactivity feedback of the core. Table 10 presents temperature reactivity feedback values for the HEU core compared to an LEU design similar to that of the Variant 1 series (same parameters as Baseline 1.0, but with Zircaloy spacers between the HEU fuel and axial reflectors). Peak fuel temperature values for each energy step are also listed, since temperature is the key limiting parameter for TREAT operation.

Table 10. Temperature Reactivity Feedback – HEU Core and LEU Baseline 1.0

	HEU			LEU		
Energy (MJ)	Core Avg Fuel Temp (°C)	Hot Spot Fuel Temp (°C)	Reactivity Change	Core Avg Fuel Temp (°C)	Hot Spot Fuel Temp (°C)	Reactivity Change
0	26	26	0.00%	26	26	0.00%
100	47.8	63.5	0.59%	47.6	61.9	0.50%
200	67.7	96.3	1.04%	67.3	93.4	1.02%
300	86.1	126	1.47%	85.7	122	1.29%
400	103.5	153.5	1.91%	102.9	148.5	1.49%
500	120	179.2	2.26%	119.3	173.4	1.96%
1000	193.2	291.6	3.83%	192.2	282	3.36%
2000	314.5	476.5	6.20%	312.8	460.6	5.49%
3000	419.2	638	8.22%	416.9	616.4	7.21%
4000	515	788.6	9.72%	512	761.2	8.65%
5000	605.2	932.9	11.10%	601.7	899.9	9.89%

5 LEU Analyses - Variant 2 Series

5.1 Initial Neutronic Evaluation

Following analysis of the Variant 1 designs, the INL design team proposed a new set of Variant 2 design options. The Variant 2 series designs feature a thicker cladding and larger fuel-to-clad gap. These design changes were intended to help prevent fuel-cladding contact and to improve the cladding's ability to withstand mechanical stress and the increased corrosion rates which accompany the higher temperatures expected if the LEU PCF is lower than the HEU PCF. Key design parameters are summarized in Table 11, and accompanying illustrations are provided in Figure 6. The Variant 2 designs were evaluated in comparison to a "Baseline" case with a thinner cladding.

Table 11. Summary of Variant 2 Design Parameters

Fuel Design	Can Corner Geometry	Clad Thickness, mils	Pre-Evacuation Fuel-Clad Gap, mils
Baseline	Chamfered	25	55
Variant 2.1	Chamfered	67.3	35.5
Variant 2.2	Chamfered	67.3	70.5
Variant 2.3	Rounded	67.3	70.5

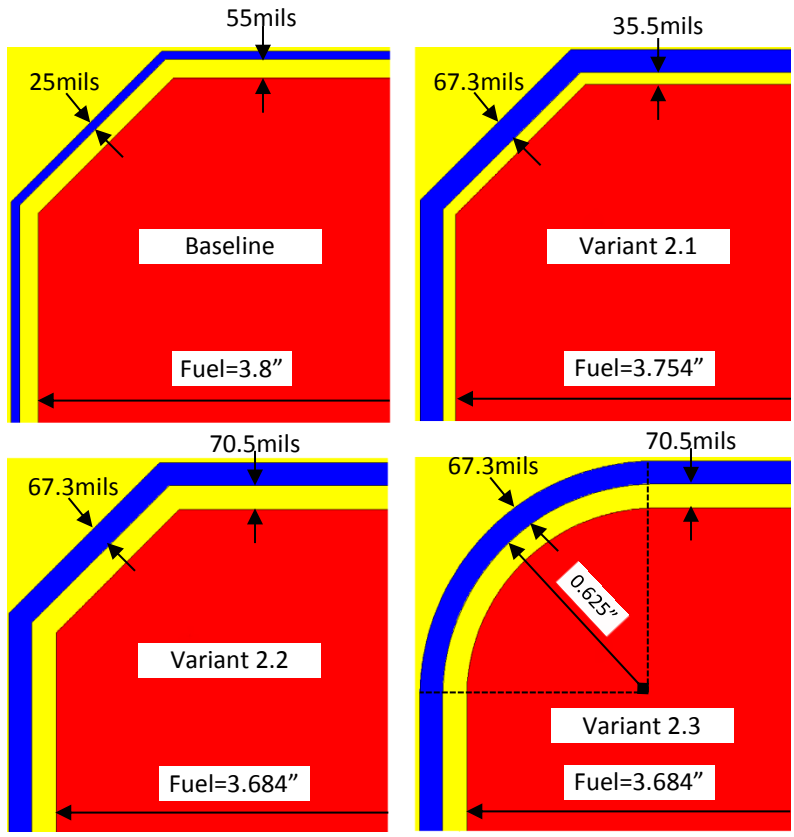

Figure 6. LEU Variant 2 Series Designs

The Variant 2 LEU designs were evaluated with a fuel C/U ratio of 1450, boron impurity of 2 ppm, 85% graphitization, and a density of 1.75 g/cm^3. As an initial step, ARO excess reactivity was calculated for each design. The results are shown in Table 12.

Table 12. All-rods-out Excess Reactivity in Variant 2 Series Designs

Fuel Design	ARO k_{eff}	Excess Reactivity	Standard FA Volume (cm^3)
Baseline	1.09684	8.83%	11026
Variant 2.1	1.02909	2.83%	10774
Variant 2.2	1.00371	0.37%	10391
Variant 2.3	1.00480	0.48%	10388

There is an administrative limit of 8% excess reactivity for the current HEU core. Therefore, assuming a similar limit for the LEU core, the composition of the Baseline case would need to be adjusted to yield a lower core loading. The Variant 2 cases all yield excess reactivity values that are too low given the core’s experimental needs. An LEU core should have enough excess reactivity to compensate for the negative reactivity of the most neutron-absorbing test vehicle and for the negative temperature reactivity in the most demanding experiment (i.e. the experiment during which the core is expected to reach the highest temperatures). Therefore, an increase in loading (i.e., decrease in C/U) would be necessary for these designs to be feasible. Because Variants 2.2 and 2.3 gave significantly lower excess reactivity than

Variant 2.1, it was determined that Variant 2.1 was the most reasonable design option. Therefore, only Variant 2.1 was evaluated in further detail neutronically.

5.2 Thermal-hydraulic Evaluation of Baseline 2.0 and Variant 2.n Designs

For each of the Variant 2 designs, a 3D thermal-hydraulic model was developed and evaluated under transient conditions with coolant flow. Additional details of each design, which are relevant to the thermal-hydraulic analysis, are provided in Table 13 and Figure 7 . The evacuation of the fuel-cladding gap during the manufacturing process is expected to cause deflection of the cladding inward. Structural analyses performed by the INL team estimated 43% (in the horizontal direction) of the cladding periphery would be in contact with the fuel under the Baseline 2.0 design. With the thicker cladding of Variants 2.1-2.3, the cladding is expected to distort but not contact the fuel. Gap dimensions before and after evacuation are included in List of Tables.

Table 13. Parameters used in the Thermal-hydraulic Evaluations of the Baseline 2.0 and Variant 2.n LEU Designs

Parameters	Baseline 2.0	Variant 2.1	Variant 2.2	Variant 2.3
Can wall corner/side properties	Chamfered	Chamfered	Chamfered	Rounded
Cladding thickness (mil)	25	67.3	67.3	67.3
Fuel/cladding gap pre-evacuation (mil)	55	35.5	70.5	70.5
Fuel/cladding gap after gas evacuation (mil)	Contact [a)]	20	55	55
Fuel length (cm)	121.91	121.92	121.92	121.92
Corner section open flow area (cm^2)	2.98	2.98	2.98	3.38
Corner section surface perimeter (cm)	6.35	6.35	6.35	11.05
Side section open flow area (cm^2)	1.59	1.59	1.59	1.33
Side section surface perimeter (cm)	31.25	31.25	31.25	26.16
Coolant flow rate per assembly (cfm)	7.48	7.48	7.48	7.48
Corner/side mass-flow ratio	22/1	22/1	22/1	20/1

[a)] *Following an evacuation of the fuel assembly, 43% of side clad wall is in direct contact with fuel meat.*

The 3D assembly models for Baseline 2.0 and Variants 2.1-2.3 were each evaluated for a 300 msec half-width temperature-limited transient generating 12.7 MJ in the hottest assembly. This transient was selected because it yields a peak fuel temperature of 600°C (the Limiting Safety System Setting – LSSS - of the HEU core) for the Baseline 2.0 design. It should be noted that in reality, different transients (with different total energy values) would be needed for each design option to match HEU core performance. An axial power profile with a peak-to-average power ratio of 1.18 was used in this analysis. A coolant flow rate of 7.48 cfm per assembly was assumed, which corresponds to a total core flow rate of 3000 cfm, with 90% of the flow flowing through the core with an equal distribution to each assembly. Peak fuel and cladding temperatures were evaluated for each design. In addition, a series of sensitivity analyses were also performed, as indicated below:

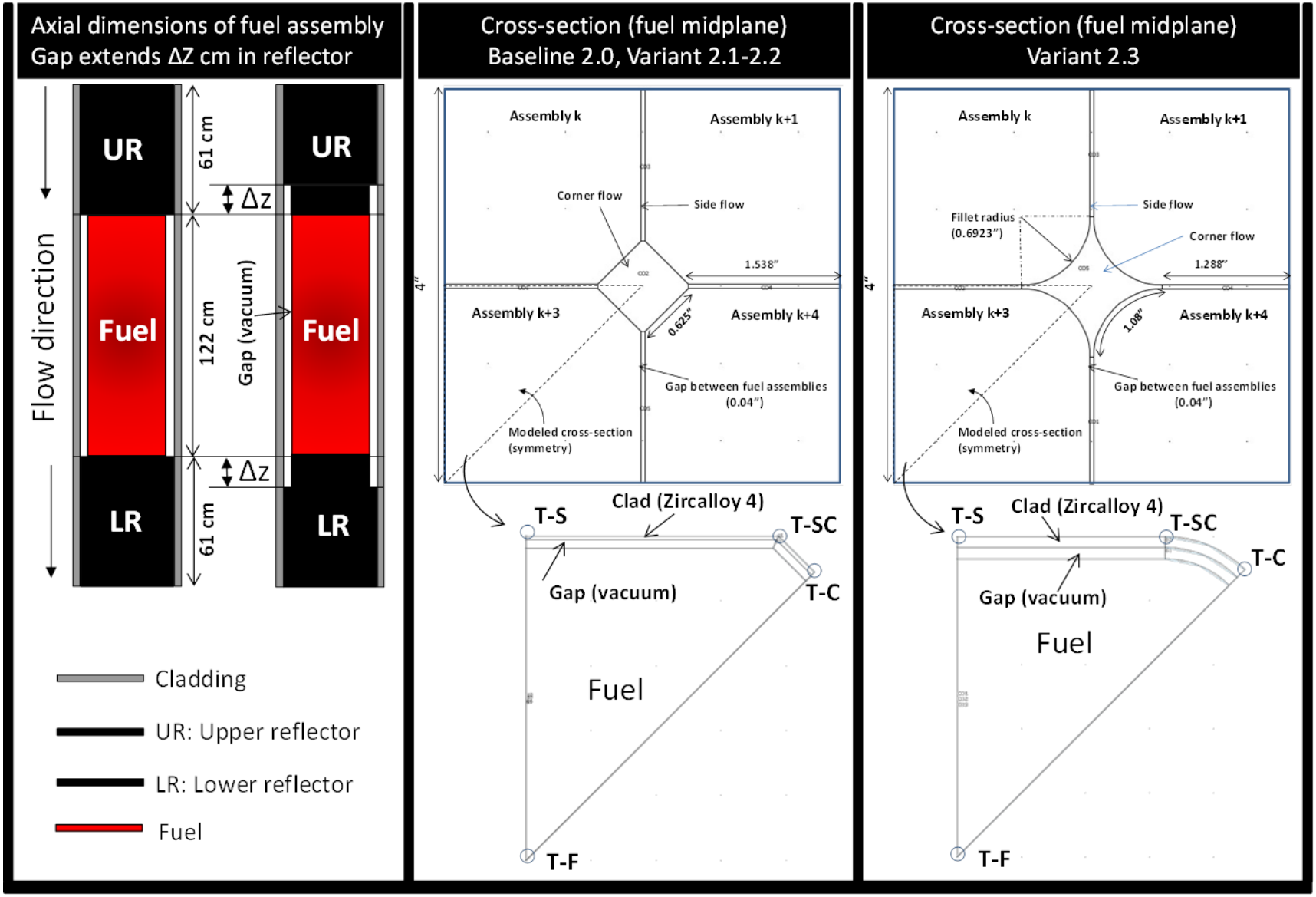

Figure 7. Axial and Cross-sectional Geometric Details of the Baseline 2.0 and Variant 2.n Designs

- The gap between the fuel and cladding also extends into the axial reflector region by a certain distance (indicated as Δz in Figure 7). The extension of the gap between the reflector and cladding was varied to investigate the impact on the axial temperature profile of the cladding. The reflector remained in contact with the fuel in all cases.
- At high vacuum quality, thermal radiation controls the heat transfer between the inner cladding surface and the fuel. The sensitivity of the peak cladding temperature to the emissivity of Zircaloy was evaluated for emissivity values in the range 0.2 – 0.4.
- Peak fuel and cladding temperatures were calculated for different total energy values (using a constant axial power profile).

5.2.1 Baseline 2.0 and Variant 2.1-2.3 Peak Fuel and Cladding Temperatures

Calculated peak fuel and cladding temperatures are provided in Table 14 for the fuel-assembly 12.7 MJ transient with cooling. Peak cladding temperatures are provided for three locations along the cladding periphery: (a) center of the side region (T_s), (b) point of intersection between the side and corner wall (T_{sc}), and (c) center of the corner region (T_c), as illustrated in Figure 8. Because the majority of coolant flow is located in the corners, peak cladding temperatures occur at the side wall (T_s).

Table 14. Peak Fuel and Cladding Temperatures for 12.7 MJ Transient with Cooling, LEU Baseline 2.0 and Variants 2.1-2.3

Region	Baseline 2.0	Variant 2.1	Variant 2.2	Variant 2.3
T_F (Fuel), °C	602	617	632	636
T_S (Cladding, far side), °C	595	517	533	514
T_SC (Cladding side/corner, °C	476	461	476	465
T_C (Cladding corner), °C	448	450	465	444
Time for peak cladding T, s	90	550	530	500

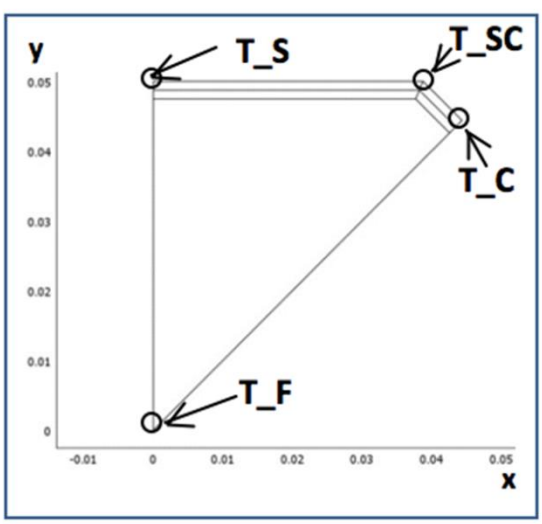

Figure 8. Locations Where Peak Cladding Temperatures were evaluated for LEU Baseline 2.0 and Variant 2.n Designs

Figure 9 highlights the peak fuel and cladding temperatures at the side. In Baseline 2.0, the side cladding is in direct contact with the fuel, and the peak cladding temperature (595°C) is therefore in near equilibrium with the peak fuel temperature. If the cladding wall was prevented from contacting the fuel for the baseline case, the peak cladding temperature would decrease to 560°C for the scenario with cooling flow present.

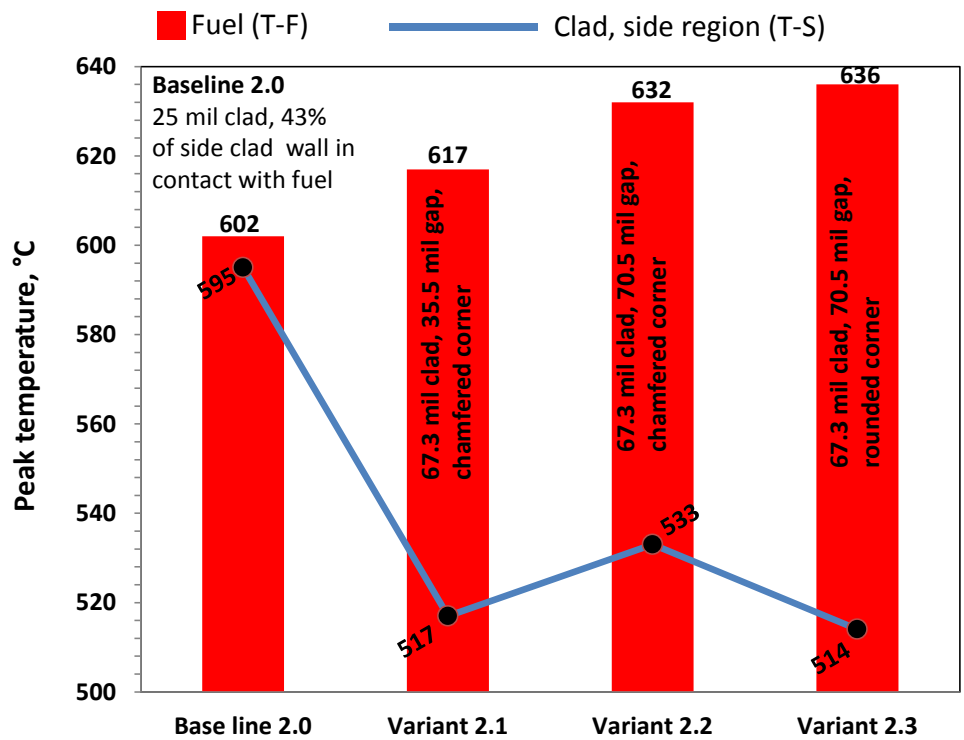

Figure 9. Peak Fuel and Cladding Temperatures at Side for 12.7 MJ Transient, Baseline 2.0 and Variants 2.1-2.3 with Cooling

5.2.2 Gap between Cladding and Reflector, Baseline 2.0 and Variants 2.n

The simulations found that the calculated peak fuel and cladding temperature values remain the same regardless of whether the reflector is in contact with the cladding or a vacuum gap is extended some distance Δz into the reflector regions. However, the axial temperature profile of the cladding is affected by the extension of the gap into the reflector.

Figure 10 shows the axial temperature profiles at the side region of the cladding (T_s) as a function of time and the extent of the gap, Δz, into the reflector. Results are presented for Variant 2.1 as an example, but the behavior would be similar for all variant cases (as long as the cladding does not contact the fuel). When there is no vacuum gap between the cladding and reflector (Δz = 0), the cladding exhibits sharp temperature peaks near the fuel-reflector interface. These peaks are exacerbated under time scales < 100 sec, when the cladding temperature is relatively cold and the graphite reflector is being heated via conduction from the fuel section. The presence of a vacuum gap between the fuel and axial reflector reduces the sharp changes in the cladding axial temperature profile, particularly for gaps extending 20 cm or greater into the reflector region.

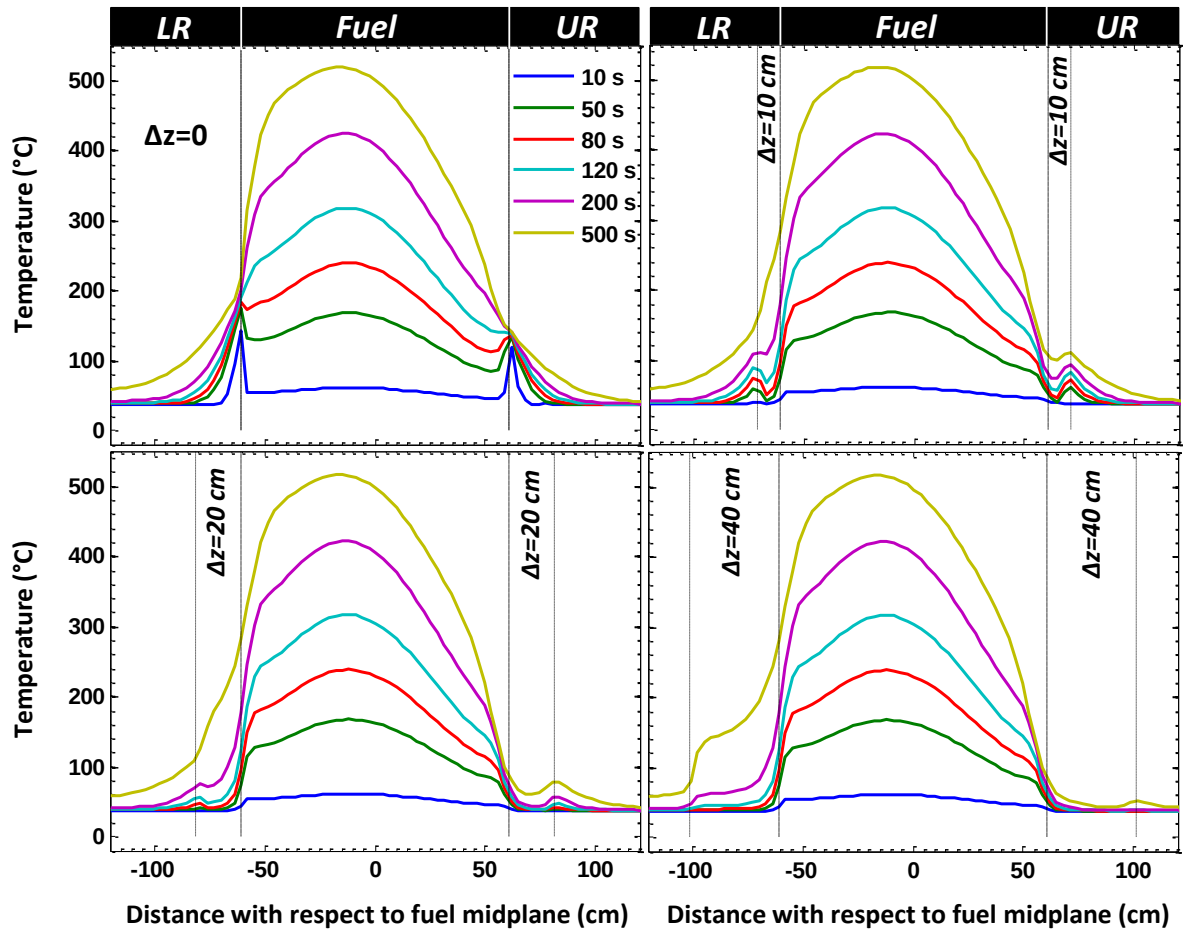

Figure 10. Temperature of the Cladding at the Side Wall as a Function of Time and Vacuum Gap Distance into the Reflector, for Variant 2.1 in a 12.7 MJ Transient with Cooling; LR = Lower Reflector and UR = Upper Reflector

5.2.3 Zircaloy Emissivity, Variant 2.1

With a high vacuum quality, thermal radiation controls the heat transfer between the inner face of the cladding and the fuel. A low Zircaloy emissivity (i.e., high reflectivity of radiant thermal energy) is beneficial to reduce the heat flux to the cladding. Base case emissivity values of 0.3 and 0.8 for the Zircaloy and fuel, respectively, were assumed in the reference thermal-hydraulic models.

The emissivity of Zircaloy-4 is strongly affected by the presence of surface oxides [13, 14]. Experimental data indicate that the emissivity of an unoxidized Zircaloy surface is constant at a value of 0.2, even at high temperatures, when evaluated under an inert atmosphere. This increases, up to a value of 0.82, when surface oxides are formed at high temperatures and steam conditions.

Figure 11 presents the effect of Zircaloy emissivity on peak cladding temperatures for the Variant 2.1 design, again for a scenario where cooling flow is present. It should be noted that given a high quality vacuum and absence of air, the inner surface of the cladding may not be affected by oxidation. Therefore, the emissivity values used in the reference model (0.3 for the Zircaloy) can be regarded as conservative. For an emissivity value of 0.2, the peak cladding temperature would be further reduced when cooling is present by almost 40°C, from 517°C to 478°C.

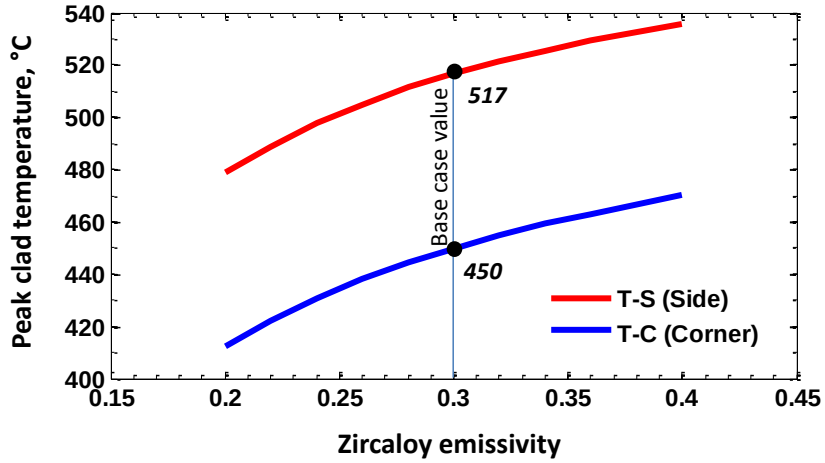

Figure 11. Effect of Zircaloy Emissivity on Peak Cladding Temperature for Variant 2.1, for 12.7 MJ Transient with Constant Peak Fuel Temperature of 617°C and Forced Air Cooling

5.2.4 Core Energy and Temperature Behavior, Variant 2.1

Baseline 2.0 and Variants 2.1-2.3 were all evaluated for the same transient total core energy. However, in reality the core energy needed to match HEU performance (i.e., HEU test sample TED) is design-dependent and is not the same in all cases. As described above, the preliminary neutronic analyses identified Variant 2.1 as the most promising design option. Therefore, a series of thermal-hydraulic simulations were performed for a set of assembly energy values (8.8 – 18.2 MJ) to develop a correlation between peak fuel and peak cladding temperature. Results are illustrated in Figure 12. For Variant 2.1, the peak fuel temperature during normal transient operations would have to be limited to ~700°C to prevent the peak cladding temperature from exceeding 600°C during normal operations with cooling.

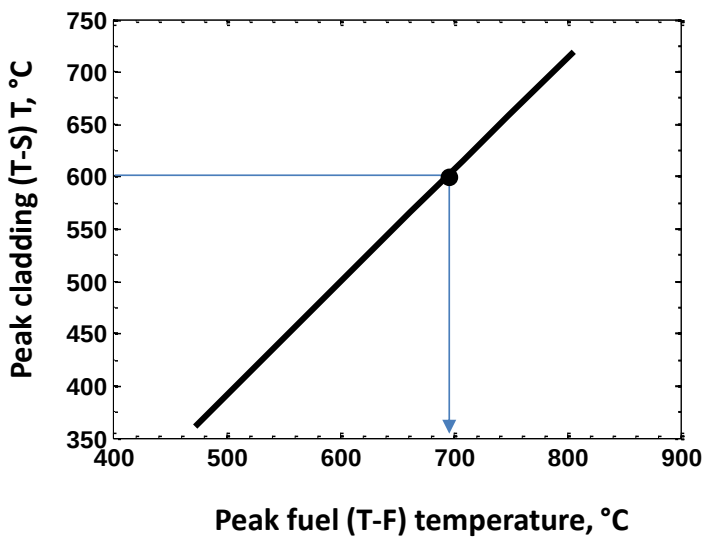

Figure 12. Relationship Between Peak Fuel Temperature and Peak Cladding Temperature, for Variant 2.1 with Cooling

5.3 Variant 2.1 Detailed Analysis

5.3.1 Variant 2.1 Summary

For further analysis of Variant 2.1, the fuel C/U was reduced from 1450 to provide a more reasonable excess reactivity. All additional simulations of Variant 2.1 were performed assuming a C/U of 1110, with 2 ppm boron, 85% graphitization, and a fuel density of 1.77 g/cm^3. ARO reactivity and rod bank worths are summarized in Table 15. All subsequent discussion of "Variant 2.1" refers to an LEU design with the Variant 2.1 geometry illustrated in Figure 6 and this updated composition.

It should be noted that the selected composition yields a reactivity which is ~1% less than the calculated reactivity of the HEU core. This was done to accommodate the decrease in control rod bank worths (compared to the HEU core) with this design, to ensure sufficient shutdown margin. For the LEU core to have larger reactivity, the uranium loading would need to be higher (decreased C/U), which would further decrease the rod worths. The reduced value of 6.51% was considered still sufficient for performing all transient experiments.

Table 15. All-Rods-Out Excess Reactivity and Control Rod Bank Worth in LEU Variant 2.1 Core

	Parameter	%Δk/k
	ARO Reactivity	6.51%
ρ_{ARO} - ρ_{In} (%)	Control	7.92%
	Transient	7.39%
	Compensation	6.83%

5.3.2 Variant 2.1 Transient Behavior

The neutronics input required by TREKIN was produced by MCNP for the Variant 2.1 LEU design. Temperature reactivity feedback is presented in Figure 13. The LEU Variant 2.1 core has significantly-lower temperature reactivity feedback compared to the HEU core. Delayed neutron fraction and prompt generation lifetime are provided in Table 16.

5.3.3 Variant 2.1 Accident Analysis

During the timeframe of this analysis, it was established by the multi-lab conversion analysis team that the LEU design evaluation must consider the zero-flow maximum accident scenario transient (as described in Section 2.3.3). Prior to this time, the analyses were focused on normal operating conditions (hence the focus on design features that enhance performance when air flow is present). Therefore, Variant 2.1 is the first design to be evaluated for the accident scenario.

5.3.3.1 Variant 2.1 Accident Analysis – Neutronic Simulations

For the M8CAL experiment vehicle and test pins, Variant 2.1 has a 26% lower PCF than the HEU core, so the total core energy for equal TED had to be determined. Following the methodology outlined in Section 2.3.3 the power-time history that would result in equal TED was calculated for the maximum shaped transient performed in HEU. The shaped transient is summarized in Table 17, and the power-time history is illustrated in Figure 14.

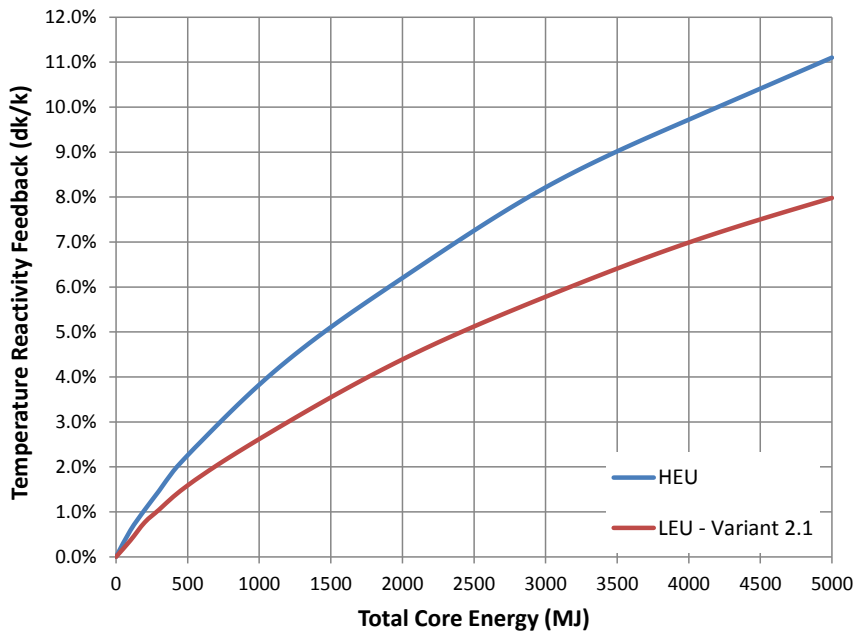

Figure 13. Temperature Reactivity Feedback vs. Core Energy for HEU and LEU Variant 2.1 M8CAL Half-slotted Core

Table 16. Kinetic Properties of LEU Variant 2.1 Core

		HEU	LEU Var. 2.1
b_i	1	0.00022	0.00023
	2	0.00114	0.00112
	3	0.00111	0.00113
	4	0.00311	0.00311
	5	0.00091	0.00089
	6	0.00032	0.00033
b_{eff}		0.00680	0.00681
L_p (μs)		860	620

Table 17. Bounding Shaped Transient, for Equal TED, in HEU and LEU Variant 2.1

	Initial Reactivity	Peak Power (MW)	Peak Fuel Temperature (°C)
HEU	5.95%	293	461
LEU	5.20%	392	533

As Table 17 shows, the maximum allowable shaped transient does not approach the core temperature limits, even in the LEU core. As discussed above, the shaped transient is instead limited by the fact that if the reactivity available prior to the transient in the HEU core were inserted as a step, the resulting power pulse would approach the 820°C accident case temperature limit. Accident scenarios for the HEU and LEU core were therefore simulated to estimate the increase in peak temperatures that could be experienced by the core with this LEU design. These results are summarized in Table 18. Because of the decrease in PCF, the LEU core exceeds the 820°C temperature limit of the HEU core. It should be noted

that the HEU fuel temperature values differ slightly from previously-reported values for this analysis. This is due to further refinement of the correlation used to represent HEU heat capacity.

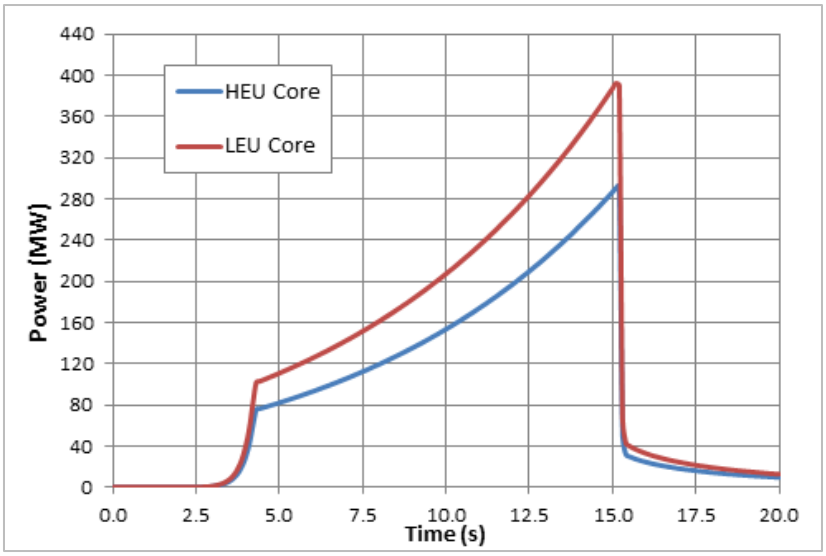

Figure 14. Maximum Shaped Transient, for Equal TED, in HEU and LEU Variant 2.1

Table 18. Behavior if Initial Available Reactivity of Bounding Shaped Transient (for Equal TED) is inserted as a Step, with no Cooling, for HEU and LEU Variant 2.1

	Inserted Reactivity	Peak Power (MW)	Energy (MJ)	Peak Fuel Temperature (°C)
HEU	5.95%	39686	4059	816
LEU	5.20%	61865	5590	958
LEU/HEU	0.87	1.56	1.38	1.20

The peak temperature in the accident scenario is directly linked to the LEU core's decrease in PCF relative to the HEU core, since this drives the reactivity needed to match the HEU core test sample TED. Using the TREKIN tables calculated for Variant 2.1, estimates of the normal and accident scenario peak fuel temperatures were developed for different LEU PCFs (relative to HEU PCF), as summarized in Table 19.

Table 19. Estimates of Peak Temperature for Different LEU/HEU PCF Values

Core (rel. to HEU PCF)	HEU	LEU (60%)	LEU (70%)	LEU (80%)	LEU (90%)
Available Reactivity	5.95%	5.95%	5.40%	4.96%	4.58%
Peak Fuel Temp. in Accident Transient (°C)	816	1133	1004	905	826
Peak Temp. in Normal Transient (°C)	461	620	554	504	463

5.3.3.2 Variant 2.1 Accident Analysis – Thermal-hydraulic Results

As calculated with TREKIN, the Variant 2.1 accident scenario is a 5.20% reactivity insertion which produces a 5590 MJ transient. Using the MCNP-calculated power distribution, the ratio of the power in the hottest assembly to total core power was determined to be 0.00429, with a maximum assembly peaking factor of 1.147 at -10.12 cm relative to the fuel mid-plane. accident scenario was evaluated. In addition, two scenarios with flow were also analyzed in order to identify the effect of cooling. Because the calculated fuel temperature exceeds the phase change temperature for Zircaloy, analyses were also performed to investigate behavior if the cladding undergoes change from α to β phase. The particular cases evaluated were:

- Case A, Cooling is present (assuming 90% of the flow capacity passes through the core, with 10% around the radial reflector, and is equally distributed among 361 assembly locations)
    - A.1: Air cooling from one blower (3000 cfm)
    - A.2: Maximum cooling, with two blowers (6000 cfm)
- Case B: No cooling is present (both blowers fail and there is no natural convection)
    - B.1: The only mode of heat dissipation is by conduction, and the cladding remains insulated from the environment (which is the scenario in the HEU SAR)
    - B.2: The only mode of heat dissipation is by conduction, and the cladding remains insulated from the environment except at the assembly end caps where there is assumed to be radiation heat transfer to an ambient temperature of 300°C.
- Case C: Zircaloy undergoes phase change, and the resultant changes in heat capacity are accounted for (using, as recommended, the properties of Zircaloy-2 [14], which are expected to be similar to those of Zircaloy-4). The heat capacity vs. temperature data used for this analysis is provided in Table 20.

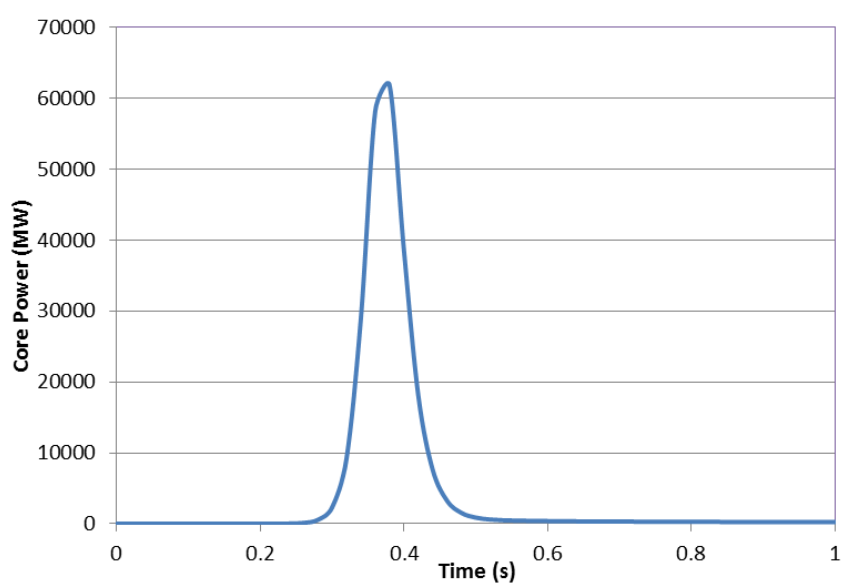

Figure 15. Power-time History of the Maximum Reactivity Insertion Accident in the LEU Variant 2.1 Core

Table 20. Heat Capacity as a Function of Temperature for Zircaloy-2

Temperature (°C)	Heat Capacity (J/kg,K)
0	283.6
27	286.4
127	296.6
227	306.9
327	317.1
427	327.3
527	337.6
627	347.8
727	358.1
827	368.3
847	370.4
867	372.9
887	393.3
907	592.3
927	1190
937	1416.6
941	1438.3
947	1335.1
967	739.3
987	385.2
1007	332.7
1027	330.2
1127	331.5

The accident scenario thermal-hydraulic results under the different evaluated conditions are summarized Table 21 and in Figure 15, showing cooling time histories to 600 °C. The time to cool to cladding temperature values of 600°C and 500°C for the cooling rates under forced convection and no-flow cases are presented in Figure 16, Table 22, and Table 23. Key observations from this analysis are as follows.

Case A – Coolant Flow Present

The analysis found that for total core flow rates of 3000 and 6000 cfm the peak cladding temperature results are 876°C and 847°C, respectively. With 3000 cfm flow, the cladding cools at a linear rate of 3.36°C/min, with a cooldown time from peak temperature to 500°C of 117 minutes. With the maximum capacity flow of 6000 cfm, the cooling increases to a linear rate of 5.29°C/minute, cooling from peak temperature to 500°C in 70 minutes. Note that peak fuel temperature remains nearly the same since assembly energy has not changed (peak fuel temperatures are established quickly, when no substantial heat loss has occurred).

Case B – No Coolant Flow

When no flow is present and the only mode of heat dissipation is conduction with the assembly insulated from the environment (i.e., the conditions of the HEU SAR), the calculated peak cladding

temperature is 918°C. The peak cladding temperature is reached after ~6 minutes, but the peak fuel temperature is reached much more quickly (after ~1 minute). At the point in time when the peak cladding temperature is reached, the cladding and fuel are at nearly the same temperature, but this temperature is approximately 40°C lower than the peak fuel temperature. Under the assumed cooling conditions, the average cladding cooling rate is 0.57°C/minute from peak temperature to 600°C (with a cooling time of 560 minutes). The cooling rate from 600°C to 500°C is strongly nonlinear, as the axial reflectors are heating. This cooling from 600°C to 500°C requires an additional time of approximately 600 minutes. The cooling rate from peak temperature to 600°C is very similar to what Freund, et al. calculated and adopted in the SAR for the HEU core [16]. Their analysis found that "the cooling rate is computed from 788°C to 649°C which occurs in 230 min. This is an average cooling rate of 0.6°C/min."

If the conditions above are maintained but the assembly end caps are no longer assumed to be insulated (i.e., radiation heat transfer is accounted for, to an ambient temperature assumed to be at 300°C), the peak cladding temperature remains at 918°C, and the average cooling rate also shows negligible change.

Case C – Zircaloy Phase Change

Despite the fact that the Zircaloy heat capacity increases significantly with phase change, the calculated peak cladding temperature showed negligible change (1°C difference) compared to the results generated assuming the heat capacity for α-phase throughout the full temperature range (which was evaluated by extrapolating the heat capacity of α-phase as a function of temperature). Therefore, from a thermal standpoint only, it can be concluded that the change in heat capacity of the cladding will not substantially affect the peak cladding temperature. This behavior is reasonable given that the thermal mass of the cladding is only a small fraction of the combined thermal mass of the fuel and reflector.

Table 21. Peak Fuel and Cladding Temperatures for Variant 2.1 Accident Scenario Under Different Conditions

Case	Coolant Flow (cfm)	Assembly Energy Density (J/cm^3)	Zr Emissivity	Zr Phase	Fuel Peak Temp (°C)	Cladding (side) Peak Temp (°C)	Cladding (corner) Peak Temp (°C)
A-1	3000	2233	0.3	α	957	876	793
A-2	6000	2233	0.3	α	957	847	701
B-1	0	2233	0.3	α	957	918	918
B-2	0	2233	0.3	α	957	918	918
C	0	2233	0.3	α, α-β	957	917	917

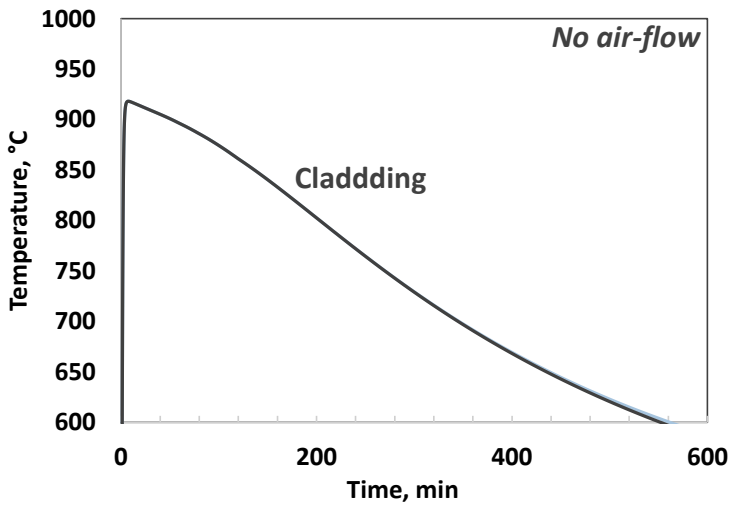

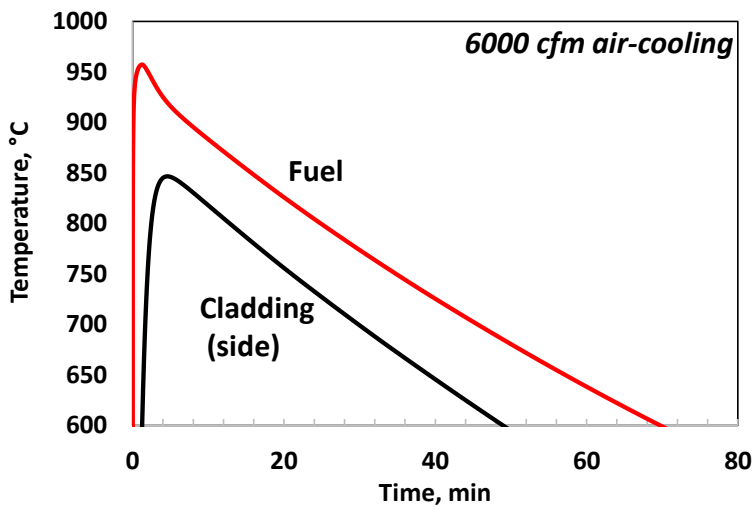

Figure 16 - Cooling Time History for LEU Variant 2.1 During an Accident-Case Scenario, With Air Flow (Upper Graph) and Without Air Flow (Lower Graph)

Table 22. Peak Cladding Temperature and Cooling Time for Variant 2.1 Accident Scenario with Coolant Flow

Case	Flow Rate (cfm)	Cladding (side) Peak Temp (°C)	Time for Peak (min)	Time for 500°C (min)	Cooling Rate to 500°C (°C/min)
A-1	3000	876	5.0	117	3.36
A-2	6000	847	4.6	70	5.29

Table 23. Peak Cladding Temperature and Cooling Time for Variant 2.1 Accident Scenario with No Coolant Flow

Case	Cladding (side) Peak Temp (°C)	Time for Peak (min)	Time for 600°C (min)	Cooling Rate to 500°C (°C/min)	Cooling Rate to 600-500°C (°C/min)
B-1	918	6.6	560	0.57	non linear
B-2	918	6.6	550	0.59	approx. 0.24

5.3.4 Steady-state Evaluation of Additional Experiments in the Variant 2.1 LEU Core

In addition to M8CAL, two other historic experiments were simulated in MCNP for the Variant 2.1 core, Test LO3 and Tests S11/S12. This was done to begin developing an understanding of how LEU performance varies over the anticipated range of future experiments possible in TREAT. For the same LEU fuel, the magnitude of the change in PCF relative to the HEU fuel may differ depending on other parameters such as the composition and geometry of the experiment vehicle and test sample, mass and fissile content of test samples, etc. Validation of the HEU models of these experiments against measured data has not yet been performed yet. Nevertheless, the simulations provide information on how LEU compares to HEU for experiments which are similar to those performed historically.

5.3.4.1 Variant 2.1 Performance for LO3

The LO3 experiment utilized a Mark-IIIA loop and test train which contained seven UK-PFR pins. These pins were annular cylinders of PuO_2-UO_2, fabricated with a Pu/(U+Pu) ratio of 0.32. The uranium was natural uranium, the plutonium contained 96.3 wt% (239Pu+240Pu), and the upper and lower breeder regions were depleted UO_2.

The actual LO3 irradiations were performed in the pre-upgrade TREAT core. However, the neutronic calculation simulations were performed assuming the upgraded core configuration, to evaluate the performance of an LEU core against the existing HEU core. An illustration of the simulated experiment vehicle and samples is provided in Figure 17. With the control rods placed at approximately critical, the LEU core showed 30% and 28% decreases in the PCF values for the peripheral and central pins, respectively, relative to values in the HEU core. There was a slight (3%) increase in the ratio of (fissions in the central pin)-to-(fissions in the peripheral pins) in the LEU core, which is reflective of the harder spectrum in the LEU core.

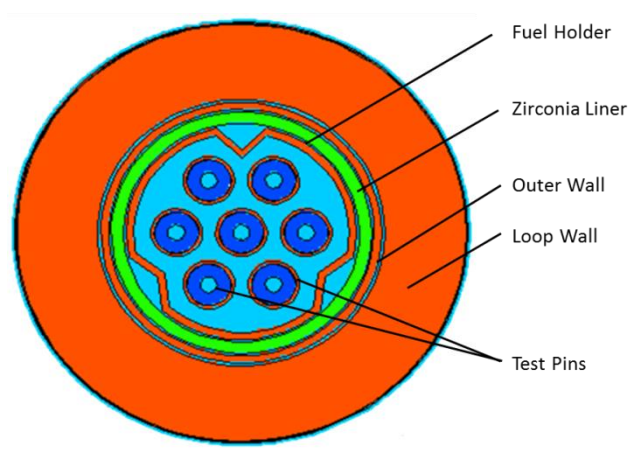

Figure 17. LO3 Experiment Configuration Used in HEU and LEU MCNP Simulations

5.3.4.2 Variant 2.1 Performance for S11/S12

Experiments S11 and S12 were single- UO_2-pin meltdown tests performed to evaluate the magnitude of fuel-coolant interaction effects. The actual experiments were performed during 1971-1972 (i.e., in the pre-upgrade core), but no data is currently available on the core loadings used. The simulations were

again performed using the upgraded core. An illustration of the MCNP model of the test pin and vehicle is provided in Figure 18. Compared to the HEU core, the PCF in the LEU core decreased by 32% to 35% for unenriched, 10% enriched, and 13% enriched UO_2 fuel pins (enrichments used in the tests).

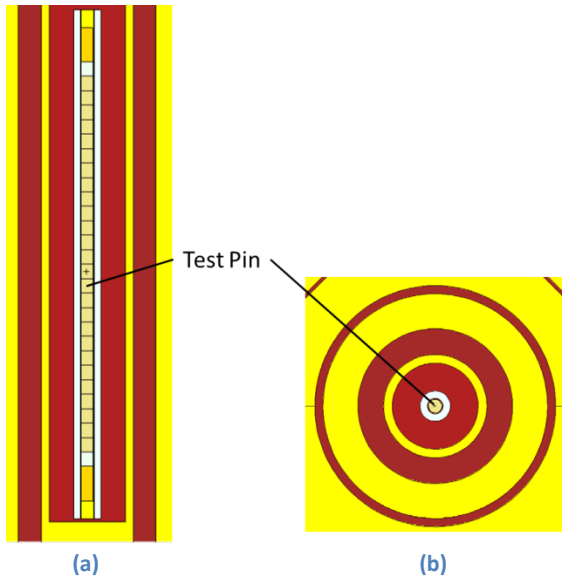

Figure 18. S11 and S12 Experiment Configuration Used in HEU and LEU MCNP Simulations, (a) X-Z View and (b) X-Y View

6 LEU Analyses - Baseline 3

The Variant 2.1 design discussed above was developed to constrain the peak cladding temperature to a lower value than the peak fuel temperature, by maintaining a gap between the fuel and cladding. The effect of the gap was found to be strongly dependent on the presence of cooling however, with a calculated peak cladding temperature 110°C lower than the peak fuel temperature with maximum coolant flow, but only 40°C lower with no coolant flow. Because the gap still reduced the peak cladding temperature somewhat relative to the fuel temperature, a set of proposed alignment options was developed by the INL team to further ensure that a gap is maintained in the hottest segment of the clad (the center of the side region). Thermal and structural evaluations of the alignment options were performed by members of the ANL and INL teams [17]. Following this structural analysis, a new design "Baseline 3.0," was proposed by the INL team which features slightly-concave surfaces along the sides of the fuel block. The Baseline 3.0 design has the same cladding thickness but a slightly reduced fuel volume compared to Variant 2.1, with a maximum side initial fuel-to-clad gap of 44 mils. The Variant 2.1 fuel specifications were maintained: fuel density = 1.77 g/cm^3, C/U = 1110, graphitization = 85%, and boron impurity = 2 ppm.

6.1 Baseline 3.0 Reference Behavior

Steady-state performance of the Baseline 3.0 design in the M8CAL half-slotted core is summarized in Table 24. PCF values were evaluated for both a high-enriched test sample (M8CAL test pin) and low-enriched test sample (hypothetical sample with the dimensions of the M8CAL pin and the composition of the low-enriched flux wires used in M8CAL), both in the M8CAL experiment vehicle and half-slotted

core loading. For comparison, the results of Variant 2.1 are listed as well. The LEU/HEU PCF ratio values are in the roughly 65-75% range. Recall from Table 19 that LEU/HEU PCF values of 60%, 70%, and 80% correspond to estimated peak fuel temperatures of 1133°C, 1004°C, and 905°C, respectively, for the Variant 2.1 design (which is very similar to Baseline 3.0). These values are significantly higher than the 820°C SL of the HEU core.

Table 24. Key Results for LEU Designs Baseline 3.0 and Variant 2.1

Parameter		Variant 2.1	Baseline 3.0
Excess Reactivity (%)		6.6	6.2
Rel. to HEU PCF – Low Enriched Target		63%	64%
Rel. to HEU PCF – High Enriched Target		73%	73%
Rod Bank Worth (%)	**Transients**	7.3	7.5
	Control/Shutdown	7.8	8.3
	Compensation	6.6	7.1

6.2 Baseline 3.0 Sensitivity Study

For further study of Baseline 3.0, perturbations to the design were evaluated for their effect on PCF, excess reactivity, and the control rod shutdown margins. The evaluated parameters are summarized in Table 25. The C/U ratio was evaluated for constant carbon atom density (atoms/barn-cm) by adjusting the uranium content. The perturbations in fuel density were evaluated assuming the relative weight fractions of the constituent isotopes were fixed. Results are presented in Table 26 and Table 27.

.

Table 25. Parameters Evaluated in Baseline 3.0 Sensitivity Study

Parameter	Current Value	Evaluated Values
C/U (total graphite constant)	1110	1099 and 1121
Graphitization	85%	80% and 90%
Boron content	2ppm	1ppm and 3ppm
Fuel density (constant wt% fractions)	1.77g/cm^3	1.72, 1.82 and 1.85g/cm^3
Enrichment (total uranium constant)	19.75 atom % (max)	19.72 atom %

Table 26. LEU Baseline 3.0 Sensitivity Study Results – Boron Impurity and Density

Affected Parameter	HEU Core	Effect on LEU Core Due to Individual Changes in Various Parameter Values					
			Boron Impurity		Density (g/cm^3)		
		Baseline	1 ppm	3 ppm	1.72	1.82	1.85
Excess (k-1)/k	7.5%	6.2%	6.7%	5.7%	5.0%	7.4%	8.2%
Transient Rod Bank Worth	9.0%	7.6%	7.5%	7.5%	7.9%	7.1%	7.0%
Control/SD Rod Bank Worth	9.3%	8.3%	7.9%	8.0%	8.4%	7.6%	7.5%
Compensation/SD Rod Bank Worth	8.5%	7.1%	6.9%	7.0%	7.2%	6.7%	6.5%
LEU/HEU PCF Ratio, High Enriched Target	-	73%	74%	73%	75%	72%	70%
HEU/HEU PCF Ratio, Low Enriched Target	-	64%	64%	65%	66%	63%	62%

Table 27. LEU Baseline 3.0 Sensitivity Study Results – Graphitization, C/U, and Enrichment

	HEU Core	LEU Core					
			Graphitization		C/U		Enrichment
		Baseline	80%	90%	1099	1121	19.72 at%
Excess (k-1)/k	7.5%	6.2%	6.3%	6.1%	6.3%	6.1%	6.2%
Transient Rod Bank Worth	9.0%	7.6%	7.5%	7.6%	7.5%	7.5%	7.6%
Control/SD Rod Bank Worth	9.3%	8.3%	7.9%	8.1%	7.9%	8.0%	8.3%
Compensation/SD Rod Bank Worth	8.5%	7.1%	6.9%	7.0%	6.9%	7.0%	7.1%
LEU/HEU PCF Ratio, High Enriched Target	-	73%	73%	74%	74%	73%	74%
HEU/HEU PCF Ratio, Low Enriched Target	-	64%	64%	65%	64%	64%	64%

The perturbations in C/U, enrichment, and graphitization were small enough that there were negligible changes in the results. Increasing/decreasing the fuel boron has minimal effect on PCF, but there is a decrease/increase in reactivity. Therefore, the C/U would need to be adjusted which would then lead to changes in PCF. A smaller boron impurity level would allow for a higher C/U which would increase PCF, while the opposite would be true for a higher boron impurity. Similarly, a lower fuel density causes a slight increase in PCF but a large reduction in reactivity, which would require a reduced C/U, leading to

lower PCFs than the reference case. On the other hand, a higher density would allow for a higher C/U and higher PCFs than the reference case.

In addition to the sensitivity study, another case was evaluated to examine the potential benefits of increasing the fuel density and the graphitization while decreasing the boron content. A summary of the composition used in this case, as compared to the reference Baseline 3.0 case, is presented in Table 28, and results are summarized in Table 29. As this analysis demonstrates, a higher density allows the fuel to achieve a similar reactivity and a higher C/U ratio which leads to an increase in PCF.

Table 28. LEU Properties Used to Investigate Further Improvement of Baseline 3.0

Parameter	Reference	Adjusted
Density (g/cm^3)	1.77	1.85
Boron (ppm)	2	1
Graphitization	85%	90%
Enrichment (%)	19.75	19.75
C/U	1110	1400

Table 29. Results Investigating Further Improvement of Baseline 3.0

Parameter		Reference	Adjusted
Excess Reactivity (%)		6.2	6.4
Transient Rod Bank Worth (%)		7.6	7.8
Control/Shutdown Rod Bank Worth (%)		8.3	8.2
Compensation Rod Bank Worth (%)		7.1	7.4
(LEU PCF) **(HEU PCF)**	**High Enriched Target**	73%	82%
	Low Enriched Target	64%	74%

6.3 Baseline 3.1 with BeO

Analyses were also performed to investigate the use of moderating elements near the test vehicle in the core, in order to improve the PCF. This work was performed for a slightly different LEU design, Baseline 3.1, which represents minor adjustments from Baseline 3.0. The design changes were made in order to match the design described in INL drawing number 604992, provided to ANL on April 14, 2015. The concept of using moderating elements near the vehicle was previously explored in the analyses outlined in Reference 1, as well as the scoping studies presented in Section 3.4. Four materials were considered in the new study: water, graphite, Be, and BeO. BeO proved the most promising and was investigated in greater detail. Two different loadings were evaluated, with 4 and 12 BeO reflectors. In each case, the fuel C/U and density were adjusted to maintain sufficient shutdown margin for each control rod bank, as indicated in Table 30 . Reactivity and rod worth results are presented in Table 31, and PCF results are

shown in Table 32. The benefits of the increased thermalization provided by the BeO are not as strong in the high enriched sample. This is thought to be due to the increased self-shielding, but further investigation is needed.

Table 30. LEU Composition for Baseline 3.1 with BeO Reflectors

	LEU-Baseline3.0	LEU - 4 BeO	LEU - 12 BeO
C/U_{total}	1110	1250	1200
Boron (ppm)	2.0	2.0	2.0
Density(g/cm^3)	1.77	1.8	1.81
Graphitization	85%	85%	85%

Table 31. Reactivity and Control Rod Bank Worths for Baseline 3.1 with BeO Reflectors

	LEU-Baseline3.0	LEU - 4 BeO	LEU - 12 BeO
Excess (ARO)	6.2%	6.4%	6.3%
Transient Rods	7.5%	7.6%	7.6%
Shutdown Rods	8.3%	8.1%	8.0%
Compensation Rods	7.1%	7.1%	6.8%

Table 32. LEU/HEU PCF for Baseline 3.0 with BeO Reflectors

Target	LEU-Baseline3.0	LEU - 4 BeO	LEU - 12 BeO
Low Enriched	64%	86%	99%
High Enriched	73%	85%	85%

Using the cold-core power distributions, estimates of the fuel hot-spot temperature values for increasing core energy are presented in Table 33. For the same amount of core energy, the loading with 12 BeO reflectors has a higher peak fuel temperature. However, as presented in Table 32, this loading also provides a larger PCF than the core with no reflectors for a high enriched target, and a larger PCF than both the core with no reflectors and the core with only four reflectors for a low enriched target. A higher PCF means that less core energy (and consequently a lower peak temperature) is needed for the same sample TED.

Table 33. Peak Fuel Temperature with Equal Core Energy, for Baseline 3.1 with BeO Reflectors

Energy (MJ)	Hot Spot Temperature (°C)		
	LEU-Baseline3.0	LEU - 4 BeO	LEU - 12 BeO
100	60.9	62.5	71.0
200	91.6	94.5	109.5
300	119.6	123.4	144.1
400	145.5	150.3	175.9
500	169.8	175.4	205.6
1000	276.1	285.4	334.9
2000	450.8	466.2	548.4
3000	603.0	624.1	736.8
4000	744.3	770.9	914.0
5000	879.4	911.5	1084.4

6.4 Baseline 3.1 with Inconel Cladding on Select Assemblies

Analyses were also performed to evaluate the use of Inconel (which can withstand higher temperatures than Zircaloy) cladding on the assemblies which experience the highest temperatures in the Baseline 3.1 core.

For a preliminary investigation of Inconel, the accident scenario peak temperature of each fuel assembly was estimated for the LEU/HEU PCF = 70% case in the M8CAL half-slotted core. Assemblies with a peak temperature above a threshold were identified as needing alternate cladding. If the threshold is set to 900°C, 47 assemblies must be changed, and if it is set to 860°C, this number increases to 71 assemblies. Initial analyses were performed changing the 47 assemblies (including two control rod assemblies) in the locations indicated in orange in Figure 1. The Inconel cladding was assumed to have a thickness of 25 mils and a density of 0.305 lb/in^3 (8.4424 g/cm^3), per the specifications in the TREAT Upgrade Core SAR. The Inconel isotopic composition is summarized in Table 34.

Table 34. Inconel Composition Used in Baseline 3.1 Cladding Analysis

Element	Ni	Cr	Fe	Mo	Mn	Si	C
Mass %	63.4%	21.5%	5%	9%	0.5%	0.5%	0.1%

Using the composition of the Baseline 3 core, the introduction of the Inconel cladding causes the ARO reactivity to decrease drastically from 6.7% to -3.8%, a 10.4% drop. To try to recover the loss in reactivity, an additional case was simulated assuming the composition of all fuel assemblies (Zircaloy- and Inconel-clad) in the mixed core of Figure 19 is changed to a "maximum" composition which approaches the manufacturing limits. This composition assumed C/U=711, density=1.84 g/cm^3, with 85% graphitization and 2 ppm boron, which yields a still-too-low reactivity of 2.7%. In addition, the very low C/U creates a much-harder neutron spectrum, decreasing both the worth of the control rods

(compensation bank decreased from 6.9% to 3.9%) and PCF (low enriched target LEU/HEU PCF decreased from 63% to 39%).

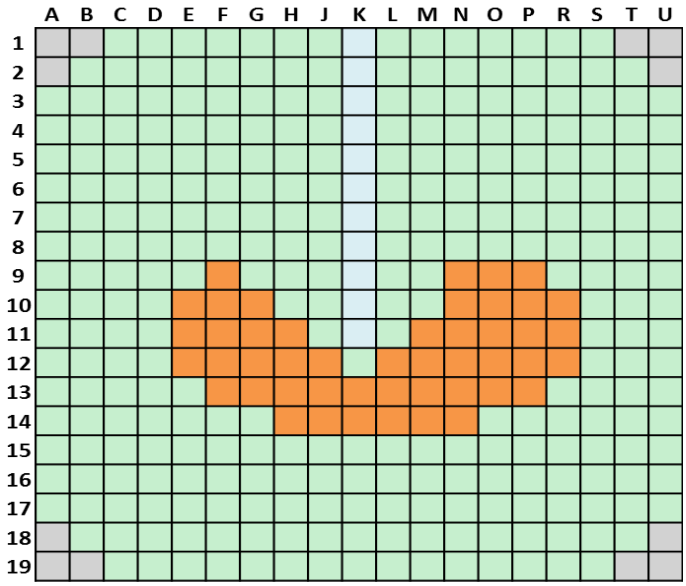

Figure 19. Locations (in Orange) where Inconel Cladding Was Tested in the Baseline 3.1 TREAT LEU Core

From this analysis, it is clear that it is not feasible to utilize Inconel on a significant number of fuel assemblies. It should also be noted that the values presented above represent the results for the scenario where 47 assembly claddings were replaced based on a 900°C temperature threshold; if 71 assemblies claddings were replaced based on an 860°C threshold, the performance would be even worse.

7 Re-baselining the LEU Design

The evolution in LEU design, from an HEU-like geometry to the design of Baseline 3, which features a thicker cladding and smaller fuel area, incorporated a number of changes that improve fuel thermal performance during normal operation (for the same amount of core energy) but do not make a significant difference in thermal performance in the zero-flow accident case. These changes also degrade the PCF. For example, Baseline 3.0 has an LEU/HEU PCF of 73% for a high-enriched target, while Variant 1.2 had a PCF ratio of 82% for the same target. Therefore, the design changes ultimately drive the peak temperatures higher, not lower. At this point in the analyses, it was therefore determined that the work should revisit a geometry that is more similar to that of the HEU assembly. In addition, it was more concretely established that a fuel density of 1.85 g/cm^3 (at the high end of the range considered) will be feasible.

7.1 June 2015 Reference Design

Using this information, a new reference design was evaluated in June 2015. This design features 25 mil thick cladding, with a 50 mil gap between fuel and cladding. The fuel is assumed to have a density of 1.85 g/cm^3, with 2 ppm boron (based on atom density ratios), and 85% graphitization. As an initial step,

three different C/U ratios were evaluated. ARO reactivity, LEU/HEU PCF (for a low enriched target), delayed neutron fraction, and prompt generation lifetime were calculated for each case (Table 35).

Table 35. Behavior of June 2015 Reference LEU Design Geometry for Different C/U Ratios

Case	C/U	Excess Reactivity	LEU/HEU PCF	l_p (x10^{-6})	b_{eff} (x10^{-3})
LEU – A	1962	8.93%	89%	890	6.9
LEU – B	2195	7.18%	95%	973	6.9
LEU – C	2470	5.14%	104%	1072	6.8

The simulations demonstrated that a higher C/U (assuming the same net fuel density) yields a lower excess reactivity, higher PCF, and longer prompt generation lifetime. It should be noted that the longer prompt generation lifetime creates a longer reactor period. This behavior will be studied in further detail later. In addition, the assumption that the density is fixed is merely an approach taken at this stage in the analysis, based on currently-available data from the fuel manufacturers. New data on the relationship between C/U and density will be incorporated in the future as it becomes available.

From this analysis, a reference case C/U value of 2150 was selected to yield roughly the same excess reactivity as the HEU core. Key results for this design are presented, compared to HEU, in Table 36, below. This LEU reference case also demonstrated significantly-larger temperature reactivity feedback compared to the Variant 2.1 and Baseline 3.0 designs, with a total feedback vs. core energy profile that is similar to that of the HEU. However, the HEU feedback comes almost entirely from the heating of the fuel graphite, while the LEU feedback is provided by both the fuel graphite and ^{238}U.

Table 36. Key Results for June 2015 LEU Reference Design with C/U=2150

		HEU	LEU
	Excess Reactivity	7.76%	7.57%
	LEU/HEU PCF, High Enriched Target	100%	96%
	l_p (x10^{-6})	867.6 ± 1.1	957.3 ± 1.3
	b_{eff} (x10^{-4})	69 ± 1	69 ± 1
Rod Worths	**Transient**	9.10%	8.77%
	Control/Shutdown	9.38%	9.28%
	Compensation/Shutdown	9.10%	8.35%

Accident analysis was performed for the LEU/HEU PCF ratio of 96%. The bounding normal-operation shaped transient (for equal TED in the LEU core as in the HEU core) is presented in Figure 20. Key results for both the shaped transient and corresponding accident temperature-limited transient are indicated in Table 37. The LEU accident generates about 11% more energy than the HEU (4413 vs. 4059 MJ). However, the peak fuel temperature in the LEU core is approximately 30 °C cooler than in the HEU core. The main reason for this is the fact that the LEU fuel has more thermal mass to absorb the energy. The higher thermal mass is due to the LEU's higher fuel density (1.85 vs 1.72 g/cm^3), slightly higher volume (up by 1.2%) and approximately 2% higher fuel heat capacity. In addition, the axial power profile for the HEU has a peak–to-average power ratio of 1.22, compared to 1.18 for the LEU.

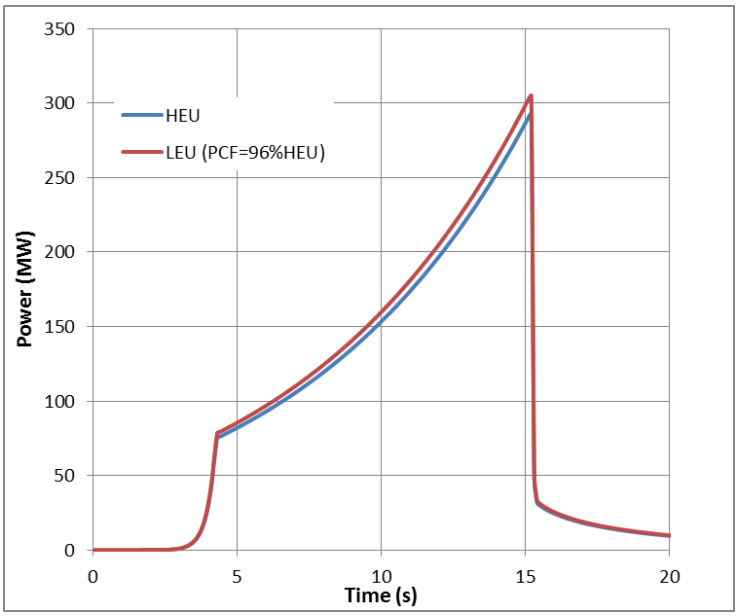

Figure 20. Bounding Shaped Transient, for Equal TED, in HEU and June 2015 LEU Reference Design

Table 37. Transient Results for June 2015 LEU Reference Design

	Bounding Shaped Transient		Accident Scenario Temperature-Limited Transient	
	HEU	LEU	HEU	LEU
Available Reactivity	5.95%	5.95%	5.95%	5.95%
Feedback	-5.93%	-5.77%	-9.80%	-10.02%
Peak Power (MW)	293	303	39686	40392
Energy (MJ)	1872	1951	4059	4413
Peak Fuel Temperature (°C)	461	427	816	787
Peak Cladding Temperature (°C)	453	420	803	775

For the accident scenario, the peak cladding temperature remains slightly cooler (12 °C） than the peak fuel temperature, despite the cladding being in direct contact with the fuel. As the cladding heats up it absorbs some heat from the fuel and therefore acts as a small heat sink. At approximately 3 minutes after the transient, the cladding and fuel are in thermal equilibrium. Assuming no flow, the cladding temperature drops below 600 °C within ~320 minutes, almost half the time required for Variant 2.1 (see Figure 20). Lower peak cladding temperatures and shorter cooling times are important to reduce corrosion rates.

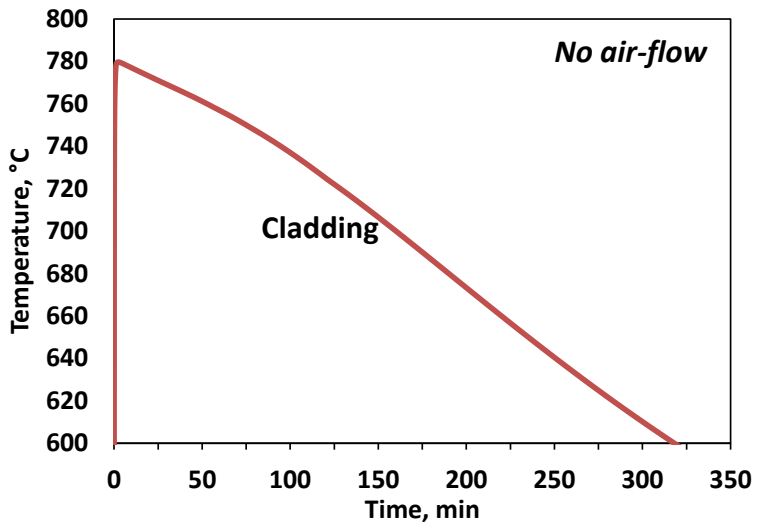

Figure 21- Cooling Time History for June 2015 LEU Reference Design During an Accident Case Scenario with No Air Flow

7.2 Perturbations of June 2015 Reference Design

The June 2015 reference design was presented in a meeting with INL and LANL on June 18, 2015. A number of design details were covered in the subsequent discussions, leading to further sensitivity studies from this design. Results of these further analyses are presented Table 38.

Table 38. Sensitivity Study of the June 2015 Reference Design

Case	Changes from June 2015 Reference Design	ARO Reactivity	(LEU PCF)/(HEU PCF)	
			Low Enriched Target	High Enriched Target
0	HEU	7.77%	100%	100%
0	LEU - Reference	7.57%	98%	96%
1	Fuel d=1.75 g/cm^3	4.85%	101%	100%
2	Fuel d=1.80 g/cm^3	6.28%	100%	97%
3	Fuel d=1.85 g/cm^3	7.62%	94%	94%
4	Fuel d=1.90 g/cm^3	8.89%	94%	92%
5	Axial reflector d = 1.85g/cm^3	7.94%	97%	94%
6	Reflector volume increased for 10 mil ref-to-clad gap	7.90%	98%	95%
7	t_{clad} increased to 35mils (fuel & ref gap = 40mils)	6.19%	97%	95%
8	Fuel volume increased for 10 mil fuel-to-clad gap	10.15%	93%	90%
9	t_{clad} increased to 35mils (fuel gap = 10 mils)	8.08%	94%	93%

Cases 1 through 4 investigated core performance for various fuel densities, assuming the same relative fractions of the constituent isotopes in all cases. For the same weight fractions, a lower density gives a higher PCF. However, lowering the density also decreases reactivity (e.g., reactivity = 7.62% for density=1.85 g/cm^3, but only 4.85% for density=1.75 g/cm^3). This means that a lower density would require a larger proportion of uranium (lower C/U) for sufficient reactivity, which would reduce the PCF, counteracting the increase in PCF due to the lower density.

A reduction in the fuel-to-clad gap (with an increase in fuel volume) leads to an increase in reactivity, as seen in Case 8. This means that if these design changes were made, a higher C/U (i.e., reduced uranium content) could be used to match the reference case reactivity. Conversely, increases in the fuel boron content reduce reactivity and would require a lower C/U to match the reference case.

8 Conclusions and Future Work

An LEU conversion of TREAT must maintain the reactor's experimental capabilities, while continuing to operate safely. Thus the converted core must be able to match the TED capabilities of the HEU core, with sufficient reactivity to perform all desired transients, while not exceeding the temperature limits of the TREAT fuel cladding.

A number of conclusions can be drawn from the LEU analyses performed over the past year and a half. In general, many of the design features which improve thermal performance during normal operation (by reducing peak cladding temperature and/or providing more material to withstand oxidation) degrade the power coupling between core and test sample. A decrease in power coupling drives both the core energy requirements and the corresponding peak temperatures higher. Figure 22 provides an example of the "trap" that can occur in trying to resolve a low LEU PCF. Developing a satisfactory LEU design requires a careful balancing of neutronic and thermal behaviors. In addition, thermal-hydraulic

simulations found that while certain design changes improve performance under normal operation, i.e., with coolant flow, they do not improve thermal performance in the zero-flow reactivity accident.

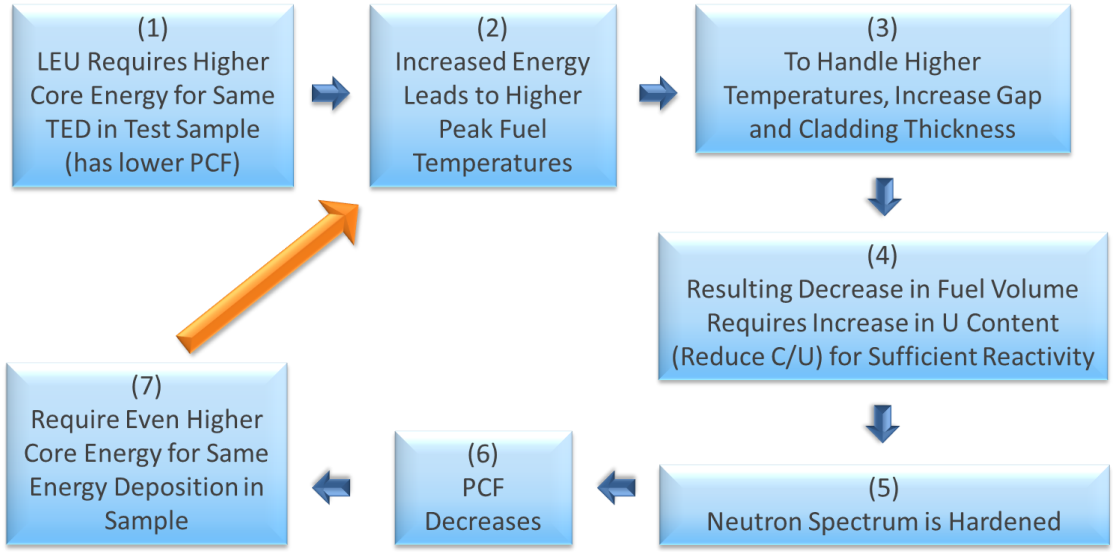

Figure 22. Illustration of the Challenge in Engineering Design Changes to Resolve LEU PCF < HEU PCF in Operations with Coolant Flow

TREAT neutronic behavior is closely tied to the neutron spectrum within the core, which is in turn linked to the C/U ratio of the fuel. In developing an LEU design, the C/U is driven by the reactivity needs of the core. If design changes are made which reduce core reactivity (examples include reducing the fuel volume, which reduces core fissile mass; increasing the gap, which increases neutron leakage; and thickening the cladding, which increases neutron absorption in that region), reactivity can only be maintained through these changes if there is an increase in uranium within the fuel – that is, a reduction in fuel C/U. A lower C/U causes a harder spectrum within the core, which both decreases the PCF and lowers the worth of the control rod banks (which can make it more challenging to maintain a sufficient shutdown margin). Conversely, a higher C/U creates a more thermal spectrum, leading to more "HEU-like" core properties.

Overall, from the LEU analyses a set of design parameters was identified which improves PCF and reduces peak fuel temperatures (bringing them close to HEU core values): (1) large fuel volume, with a small gap and thin cladding, (2) high C/U ratio (which creates a more thermal spectrum), and (3) high density, which makes a high C/U possible and also provides greater thermal mass for a given amount of energy. As the LEU analysis work outlined above was performed, the INL and LANL fuels team continued to work on determining manufacturing capabilities and limitations. Using knowledge gained in both the computational analysis and the manufacturing developments, a new LEU baseline design has largely been established. This new design will be analyzed in detail in a subsequent report.

References

1. Kontogeorgakos, D., K. Derstine, A. Wright, T. Bauer, and J. Stevens, "Initial Neutronics Analyses for HEU to LEU Fuel Conversion of the Transient Reactor Test Facility (TREAT) at the Idaho National Laboratory", ANL/GTRI/TM-13/4, Argonne National Laboratory, June 2013.

2. D. Papadias and A. E. Wright, "Thermal Analysis of a TREAT Fuel Assembly", ANL/GTRI/TM-14/14, Argonne National Laboratory, July 2014.

3. D. Kontogeorgakos, H. Connaway, G. Yesilyurt, and A. E. Wright, "Neutronic Analysis of the Minimum Original HEU TREAT Core", ANL/GTRI/TM-14/13, Argonne National Laboratory, April 2014.

4. W. R. Robinson and T. H. Bauer, "The M8 Power Calibration Experiment (M8CAL)", ANL-IFR-232, Argonne National Laboratory, 1994.

5. X-5 Monte Carlo Team, "MCNP – A General N-Particle Transport Code, Version 5 – Volume I: Overview and Theory", LA-UR-03-1987, Los Alamos National Laboratory, April 2003.

6. D. C. Kontogeorgakos, H. M. Connaway, A. E. Wright, G. Yesilyurt, K. L. Derstine, M. D. DeHart, and S. R. Morrell, "Neutronics Analyses for an LEU Core for TREAT", Transactions of the American Nuclear Society, Vol. 111, pp. 1248-1251, Anaheim, California, November 9-13, 2014.

7. K. L. Derstine, T. H. Bauer, D. Kontogeorgakos, and A. E. Wright, "TREKIN/ANL Software Users Guide", ANL/GTRI/TM-13/2, Argonne National Laboratory, February 2013.

8. D. Kontogeorgakos, H. M. Connaway, and A. E. Wright, "TREAT Transient HEU Core Analysis Benchmarking", ANL/GTRI/TM-14/11, Argonne National Laboratory, May 2014.

9. D. C. Kontogeorgakos, H. M. Connaway, K. L. Derstine, and A. E. Wright, "Temperature Limited Transient Calculations for the Transient Reactor Test Facility (TREAT) Using MCNP and the Point Kinetics Code TREKIN", ANS MC2015 – Joint International Conference on Mathematics and Computation (M&C), Supercomputing in Nuclear Applications (SNA), and the Monte Carlo (MC) Method, Nashville, TN, April 19-23, 2015.

10. F. Brown, "The makxsf Code with Doppler Broadening", LA-UR-06-7002, Los Alamos National Laboratory, April 2003.

11. K. Mo, D. Yun, A. M. Yacout, and A. E. Wright, "Heat Transfer Simulations of the UO_2 Particle-Graphite System in TREAT Fuel", Nuclear Engineering and Design 293 (2015) 313-322, August 2015.

12. D. C. Kontogeorgakos, H. M. Connaway, and A. E. Wright, "Temperature Dependence of Test Fuel Power Density and Core Energy during Transient Reactor Test Facility (TREAT) Irradiation Experiments", Transactions of the American Nuclear Society, Vol. 112, pp. 363-366, San Antonio, Texas, June 7-11, 2015.

13. E. V. Murphy and F. Havelock, "Emissivity of zirconium alloys in air in the temperature range 100-400C," *Journal of Nuclear Materials*, vol. 60, pp. 167-176, 1976.

14. P. M. Mathew and I. M. George, "Total emissivity of Zircaloy-4 at high temperatures," in *17th Annual Canadian Nuclear Society Conference*, Fredericton, NB (Canada), 1996.

15. International Atomic Energy Agency, "Thermo-physical Properties Database of Materials for Light Water Reactors and Heavy Water Reactors," International Atomic Energy Agency, IAEA-TECDOC-1496, 2006.

16. G. A. Freund, P. Elias, D. R. MacFarlane, and J. D. Geier, “Design Summary Report on the Transient Reactor Test Facility (TREAT)”, ANL-6034, June 1960.

17. B. D. Coryell, I. Van Rooyen, D. Papadias, P. Strons, A. Crawford, and A. E. Wright, “Graphite Fuel Block Alignment Options to Mitigate Adverse Thermal and Structural Stress Behaviors”, ASME Power & Energy 2015, San Diego, California, June 28 – July 2, 2015.

Nuclear Engineering Division
Argonne National Laboratory
9700 South Cass Avenue, Bldg. 208
Argonne, IL 60439-4842

www.anl.gov

Argonne National Laboratory is a U.S. Department of Energy
laboratory managed by UChicago Argonne, LLC